

JAERI-M

8 4 8 3

AN ANALYSIS OF CSNI STANDARD PROBLEM
NO.6 BY ALARM-B I COMPUTER CODE

October 1979

Shinobu SASAKI

この報告書は、日本原子力研究所が JAERI-M レポートとして、不定期に刊行している研究報告書です。入手、複製などのお問い合わせは、日本原子力研究所技術情報部（茨城県那珂郡東海村）あて、お申しこしください。

JAERI-M reports, issued irregularly, describe the results of research works carried out in JAERI. Inquiries about the availability of reports and their reproduction should be addressed to Division of Technical Information, Japan Atomic Energy Research Institute, Tokai-mura, Naka-gun, Ibaraki-ken, Japan.

AN ANALYSIS OF CSNI STANDARD PROBLEM
NO.6 BY ALARM-B1 COMPUTER CODE

Shinobu SASAKI

Division of Reactor Safety Evaluation,
Tokai Research Establishment, JAERI

(Received September 14, 1979)

Presented in this report are the results of a computer simulation of the CSNI International Standard Problem NO.6 (ISP6) by the ALARM-B1 code.

The aim of this standard problem is particularly to examine the capability of analytical models relating to the two-phase mixture level and the discharge mass flow rate using the individual participants' computer codes.

The theoretical predictions were performed to explore the separate effects during the initial three seconds attended with a non-equilibrium physical phenomenon.

The ISP6, which is based on the Battelle Frankfurt experiment duplicating a BWR steam line break accident, might not be appropriate as a bench mark problem of the ALARM-B1 program (version 2), because it contains an unreasonable demand treating a thermal non-equilibrium process with an equilibrium model.

Apart from the pressure history arising from the non-equilibrium feature, the transient steam-water interface in the vessel was tracked sufficiently by using the bubble-rise-model incorporated in the ALARM-B1 code. In addition, the calculated mass flow rate at the exit plane during the steam phase blowdown was correct within the 15 % experimental error bands.

Key words

NEA-CSNI, Standard Problem, ALARM-B1 Code, BWR-LOCA, Bubble-rise Model, Non-equilibrium Phenomenon, Carry-over, Flashing, Slip, Metastable, Entrainment

計算コード ALARM-B 1 による CSNI 標準問題 No. 6 の解析

日本原子力研究所東海研究所安全解析部

佐々木 忍

(1979年9月14日受理)

BWR用 LOCA 解析コード ALARM-B 1 による CSNI 国際標準問題 No. 6 の解析結果をまとめたものである。問題の趣旨は、特にブローダウン後の液位上昇や流出流量を計算するモデルの妥当性を検証することにおかれた。今回の計算は、非平衡現象が存在する初期の phase に対して実行された。西ドイツ Battelle 研究所で実施された本実験は、平衡モデルの計算コードにより非平衡現象を解明しようとする無理があるため、本コードのサンプル問題としては、必ずしも適当ではないが、当該コードによる解析結果が、実際の非平衡現象にどの程度肉薄するものか注目された。压力容器内での非平衡性による圧力の一時的不一致がみられたが、後半に両者は近づいた。液位の上昇は、コードのもつ分離モデルでよく説明され更に流出流量も 15% の実験誤差範囲内で、ほぼ正しく予測された。

Contents

1. Introductory Remarks	1
2. Experimental Facility Description	6
3. Brief Description of ALARM-B1 Code	11
4. Simulation Model of ALARM-B1 Code	13
5. Results and Discussions	18
5.1 Pressure History	19
5.2 Temperature History	23
5.3 Liquid Level History	24
5.4 Discharge Mass Flow Rate History	26
6. Summary	29
7. Concluding Remarks	31
Acknowledgment	33
References	34
Appendices	65

目 次

1. 序言	1
2. 実験装置の説明	6
3. ALARM-B 1 コードの概要	11
4. 計算モデル	13
5. 計算結果とその検討	18
5.1 圧力挙動	19
5.2 温度挙動	23
5.3 液位挙動	24
5.4 流出流量挙動	26
6. 要約	29
7. 結言	31
謝辞	33
参考文献	34
付録	65

1. Introductory Remarks

OECD NEA Standard Problem NO.6 was adopted at the fourth meeting of the CSNI (Committee on the Safety of Nuclear Installations) Ad Hoc Working Group on Emergency Core Cooling in December 1976.

It is based on one of a series of multifarious vessel blow-down tests already carried out at the Battelle Institute in Frankfurt (May, 1976) in order to study a hypothesized loss-of-coolant process following the rupture of a pipe. These tests series were designed to investigate the fundamental thermal-hydraulic phenomena pertaining to the decompression process of two types of light water cooled reactors; PWR (Pressurized Water Reactor) which contains hot subcooled water only, and BWR (Boiling Water Reactor) which contains saturated water in the vapor region. The present experiment called SWR-2R TEST simulates an instantaneous 100 % main steam line rupture of BWR accidents. During the blowdown, the power was not supplied because of the isothermal test condition. The main objectives of this standard problem were to check the water level and the discharge flow models in existing computer codes, and in addition, to scrutinize the behaviors of the coolant pressure and temperature at the specified locations.

The ISP6 was defined as the open-type problem; that is, all the participants know the results of the experiment in question before their analyses.

Especially interest was centered around the non-equilibrium phenomenon during the early period of the depressurization as a separate effect test.

From the viewpoint of the code analysis, it was also of concern how far the non-equilibrium state can be explained in terms of the current analytical model. The computer program employed in the analysis of the CSNI LOCA standard problem 6 was the ALARM-B1 and the computation was executed on a FACOM-230/75 computer. So far, checkout runs for this code have been scarcely performed because appropriate sample problems or published experimental data were missing. In the prediction of the proposed experiment, it was considered to be an unreasonable calculational exercise for an early phase analysis of blowdown by the equilibrium code such as the ALARM-B1, since there existed a noticeable non-equilibrium characteristics in the vessel. Hence, there was no reason to expect that the predictions would trace the experimental behaviors thoroughly. The most fundamental properties of the code used were to assume a thermal equilibrium between the two phases.

Although any physical models with respect to a non-equilibrium are not introduced in the ALARM-B1 code, checkout runs was done as a good chance to assess the validity or applicability of this code. This report presents a short description of the experimental apparatus and of the ALARM-B1 applied and system modelling, input data and results for the calculation. Including comparisons with some extracted results of the top blowdown experiment, a brief discussion was given about their individual areas of an agreement and also a disagreement.

A disagreement provides, in general, a useful information to analytical model development and improvement as a basis for the verification of codes. The lack of agreements was evidenced

in the pressure data or the incipient water level. After disappearance of the non-equilibrium phenomenon in the pressure vessel, the prediction gradually tends to agree with results of test. Three seconds later, the two was nearly in the agreement. That is to say, it might be expected that this code is capable of predicting the system behaviors adequately within a stabilized saturation regime. It was confirmed that a marked difference of the pressure in the initial phase was the discrepancy caused by the modelling limitations. Also, the bubble-separation model in the ALARM-B1 made the water level rise reasonably.

This calculation has required CPU Time 102 seconds for physical time 3.75 seconds.

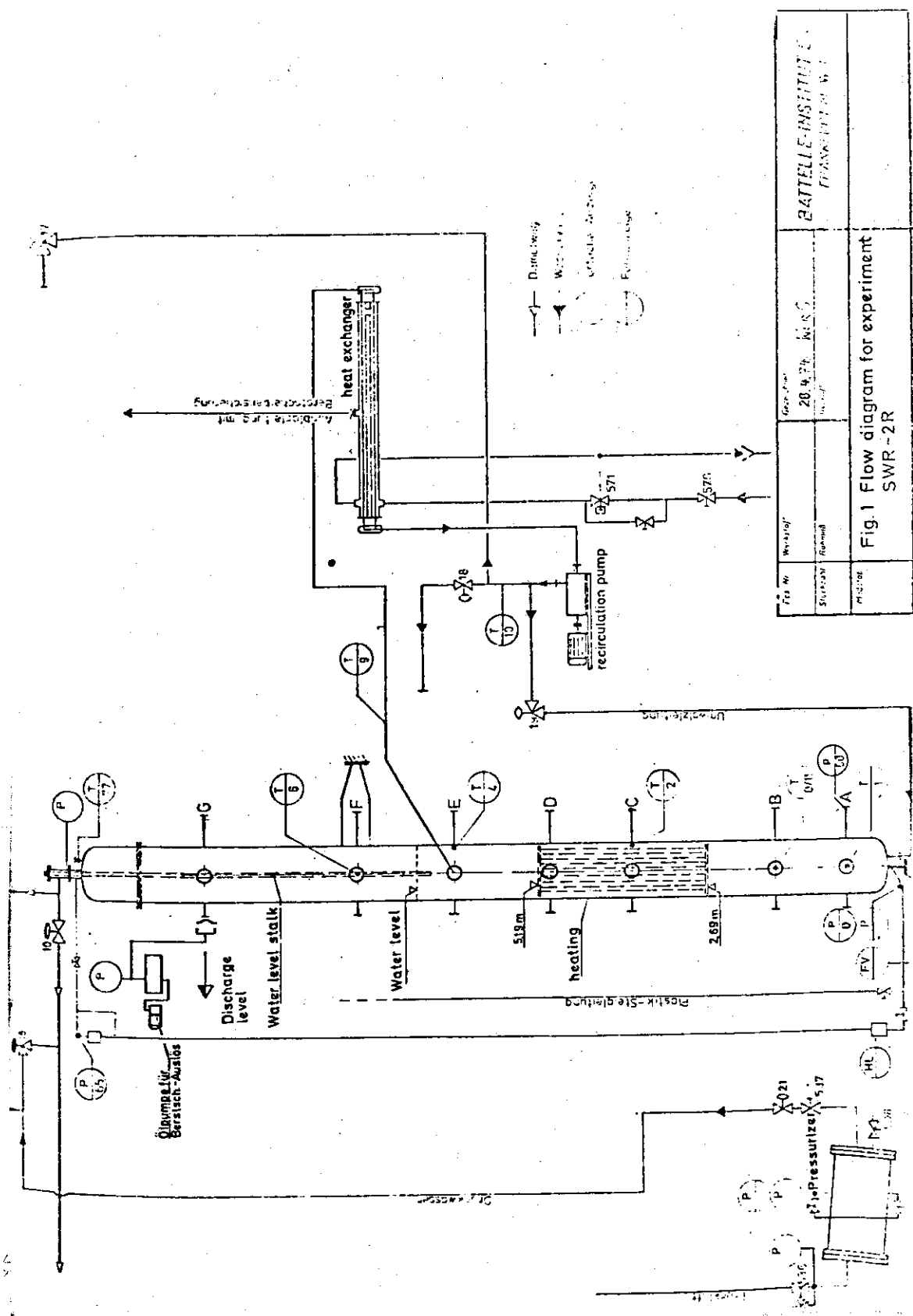


Fig. 1 Flow Diagram for Experiment SWR-2R

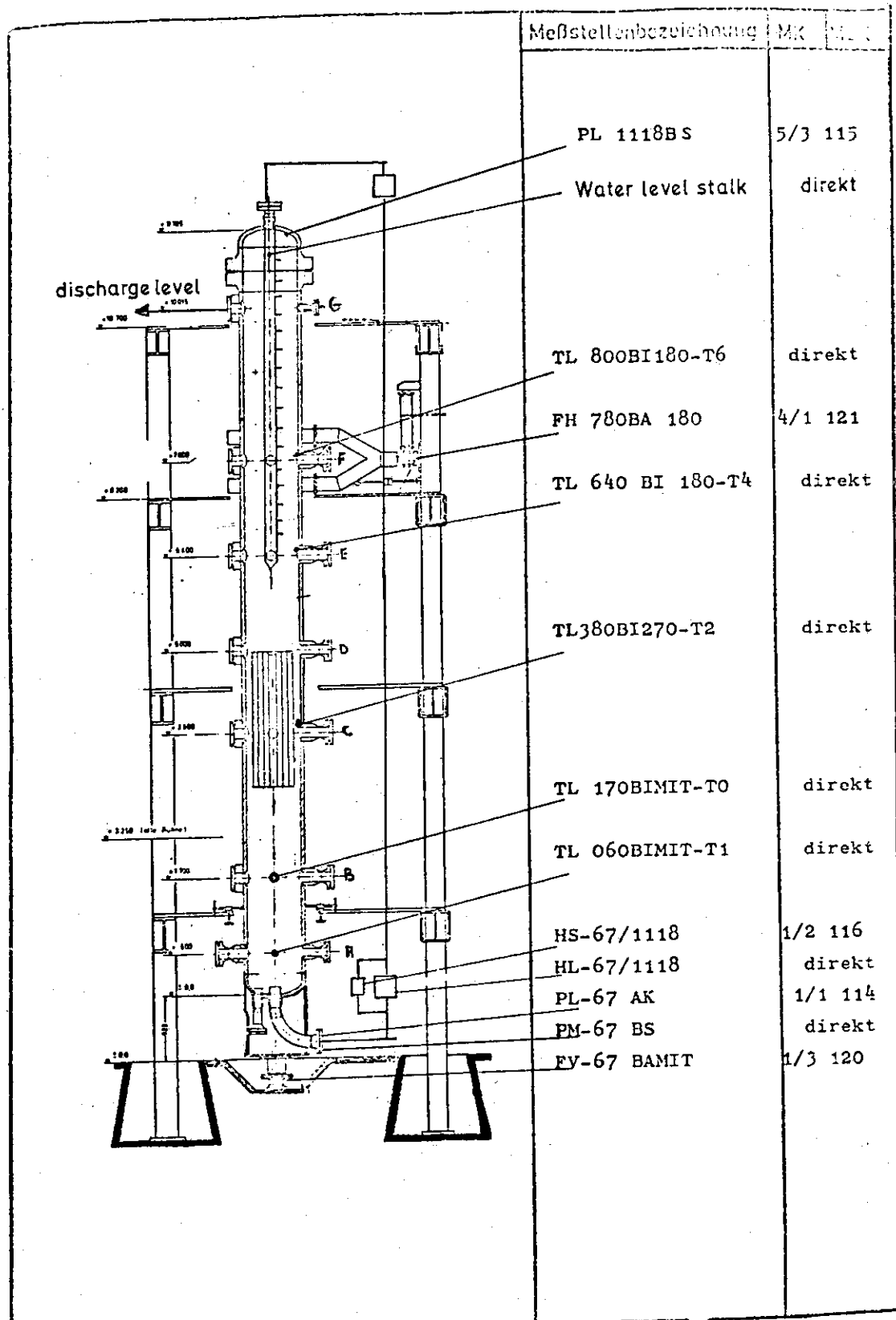


Fig. 2 Pressure Vessel with Supporting Frame Work

2. Experimental Facility Description

Safety studies simulating the discharge process after a postulated piping rupture of a BWR were conducted in a simple vessel. Figures 1 to 2 represent the schematic view for the SWR-2R experimental reactor simulator.

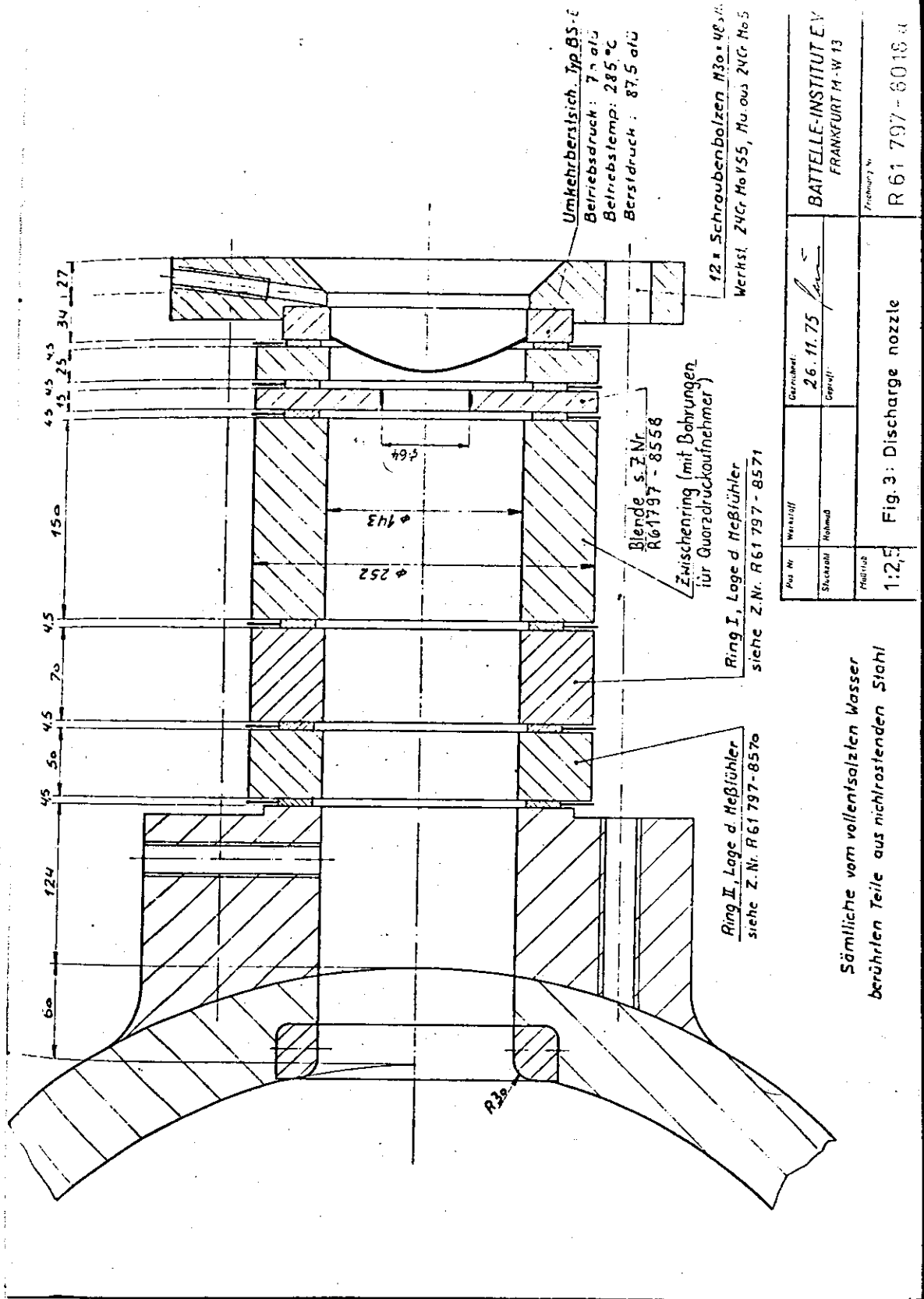
The full description of the facility is given in the reference. (1)*

In short, this vessel has an inner diameter of 0.77 m, a volume of 5.2 m³ and a height of 11.19 m, which is almost the height of a commercial power reactor core. In the middle of the vessel, there is only a simulated core (2.5 m in effective length) with electrical resistance heating. The test was made with pressure vessel with no internals.

The heater furnishes an electrical power (about 600 KW), which is necessary to adjust the incipient water temperature distributions in the pressure vessel. The heating is then turned off, when the desired temperature was established. The nozzles at the six different elevations A to G indicated in the figure, are equipped in order to perform the blowdown simulation tests for both a PWR and a BWR under the various conditions.

One of them was used as a break nozzle and at the other elevations the measurements of the pressure and the temperature were made. The discharge nozzle for the run SWR-2R was located at the level G, 10.015 m above the vessel base. The configuration of the nozzle is shown in Fig.3. As such, the experiment in question was done to simulate the main steam line rupture of BWR's. The break was simulated by the orifice behind the

* References are associated with numbers in brackets.



Pos. Nr.	Werkstoff	Gezeichnet	BATTELLE-INSTITUT E.V.
Stückzahl	Normmaß	26.11.75	FRANKFURT M-W 13
Material			Zeichner
1:2,5			R 61 797 - 8018 a

Fig. 3 Discharge Nozzle

concave rupture disc. In this isothermal test, a sharp edged orifice plate with an inner diameter of 64 mm was installed to the steam line duct. By destroying this rupture disc, a LOCA experiment is started. High pressure two-phase flow behaviors were observed through the fluid discharge from a top nozzle in the steam zone. The measurement instruments of the temperature and the pressure are indicated in Table 1. Additionally, the pressure gauges in the nozzle were measured at the eight different positions, while the temperature gauges at the four locations. The measurement of the fluid temperature was made by means of the two types of gauges — "slow resistance thermometers" and "fast thermoelements" —: the former is installed to control the stationary temperature stratification while the latter to measure the transient temperature.

The fluid density in the nozzle was determined from γ -ray absorption method. The discharge mass flow was determined from the density results and drag force measurement. The accuracy of the mass flow rate data was reported to be within approximately 10 through 15 %.

Transient liquid level was observed by a stalk equipped with electrical contacts. When the water level wets a contact, current flows between the electrodes, producing the electrical signals. It has ± 2 cm measurement errors. The principal initial conditions specified for the problem are the following:

Pressure	71.1 bar	at the position PL-67 AK
Temperature	285.5 °C	at the position A (TL-060-BIMIT)
	289.4 °C	at the position B (TL-170-BIMIT)
	289.5 °C	at the position C (TL-380-BI270)
	288.0 °C	at the position E (TL-640-BI180)
Water level	7.07 m	above the vessel base (285 °C water temperature)

They are made to be within a range of the typical reactor condition to investigate the various effects arising from the blowdown.

Level	Pressure Gauge	Temperature Gauge	
		(Slow)	(Fast)
A	PS060 BIMIT	TL060 BIMIT	TS060 BIMIT
B	PS170 BI000 PS170 BI180	TL170 BIMIT	TS170 BI000 TS170 BI180
C	PS380 BI000 PS380 BI180	TL380 BI270	TS380 BI000 TS380 BI180
E	PS640 BI000 PS640 BI180	TL640 BI180	TS640 BI000 TS640 BI180
F	PS780 BI180	TL800 BI180	TS780 BI180
G	PS999 BI180		TS999 BI180
Relative accuracy	~ 1 %	~ 1 °C	~ 2 °C

Table 1 Measurement Instrument of Pressure and Temperature

3. Brief Description of ALARM-B1 code

The calculation procedure for predicting the thermal-hydraulic response of the BWR LOCA with a large break has been newly developed for the FACOM-230 series in JAERI. This code ALARM-B1 is a one-dimensional node and junction type (lumped parameters) loop code in which the heat transfer from the fuel rod to the fluid during the blowdown is provided by input data.

In the calculation model, the primary reactor system of current GE type BWR's with jet pumps is simulated by some control volumes with junctions.

Based on the thermal equilibrium assumption, the one dimensional mass, energy and momentum conservation equations are solved in the individual volume nodes simultaneously. At the present version Update 2, the momentum flux term is neglected in the flow equation. Concerning to the hydrodynamics in the control volumes, the selection as to whether homogeneous or separate is quite optional as in ALARM-P1.⁽¹³⁾ No slip between the phases is taken into account for the present. For the jet pump behavior, the conservation equations are solved for six cases in accordance with whether the drive, suction and throat flow are in the normal or reverse flow condition. The characteristics of the recirculation pump is calculated by the homologous law using a set of input performance curves.

At the present stage, the heat transfer in the core region is treated in detail by another code (e.g., HYDY). That is, the ALARM-B1 only presents the boundary conditions at the core inlet and outlet. The details of ALARM-B1 are treated in the code manuals.⁽²⁾

In the program, a calculational frame work in modelling, such as the transient heat transfer or ECCS problem is still under way. Furthermore, premature parts in this code as the ECCS evaluation code are the major tasks to be improved as soon as possible.

As an extension of current version, above problems will be self-contained in the forthcoming version ALARM-B2.

4. Simulation Model for ALARM-B1 code

The ALARM-B1 noding diagram used to carry out the computation for the Standard Problem NO.6 is shown in Fig.4.

As is seen, the pressure vessel was divided into three control volumes with three junctions. A very simple nodarization scheme was accepted here, though several different proposals have been tried in modelling of experimental equipment. The initial water depth in the vessel is 7.07 m, which is above the region 2 (control volume 2). The discharge nozzle connected to the vessel was ignored in modelling because of a small volume.

A rupture has started the blowdown at time 0.0001 seconds. It was treated as a leak junction and simulated by a 64 mm diameter orifice at 9.96 m above the bottom of the pressure vessel. Leak data were input as a function of time vs. fluid cross section. The sink pressure was assumed to be atmospheric.

A multiplier for the Moody's two-phase critical flow model was set to 0.75. It is an arbitrary number to adjust the maximum flow through the discharge nozzle.^{(7) (8)} A bubble rise model applied only to the control volume 3 was determined from $ALPH = 2.0$ for a bubble slope parameter (density gradient) and $VBUB = 4$ (ft/sec) for a bubble escape velocity⁽²⁾ (a bubble data submitted to CSNI). A value of 1.0 for the bubble density gradient stands for a homogeneous mixture. The velocity is the rate of separation of the rising vapor bubbles into the steam dome. The other nodes were assumed to be homogeneous in order to avoid the physical inconsistency called "layer cake situation".

It should be noticed that the separation models in vertically

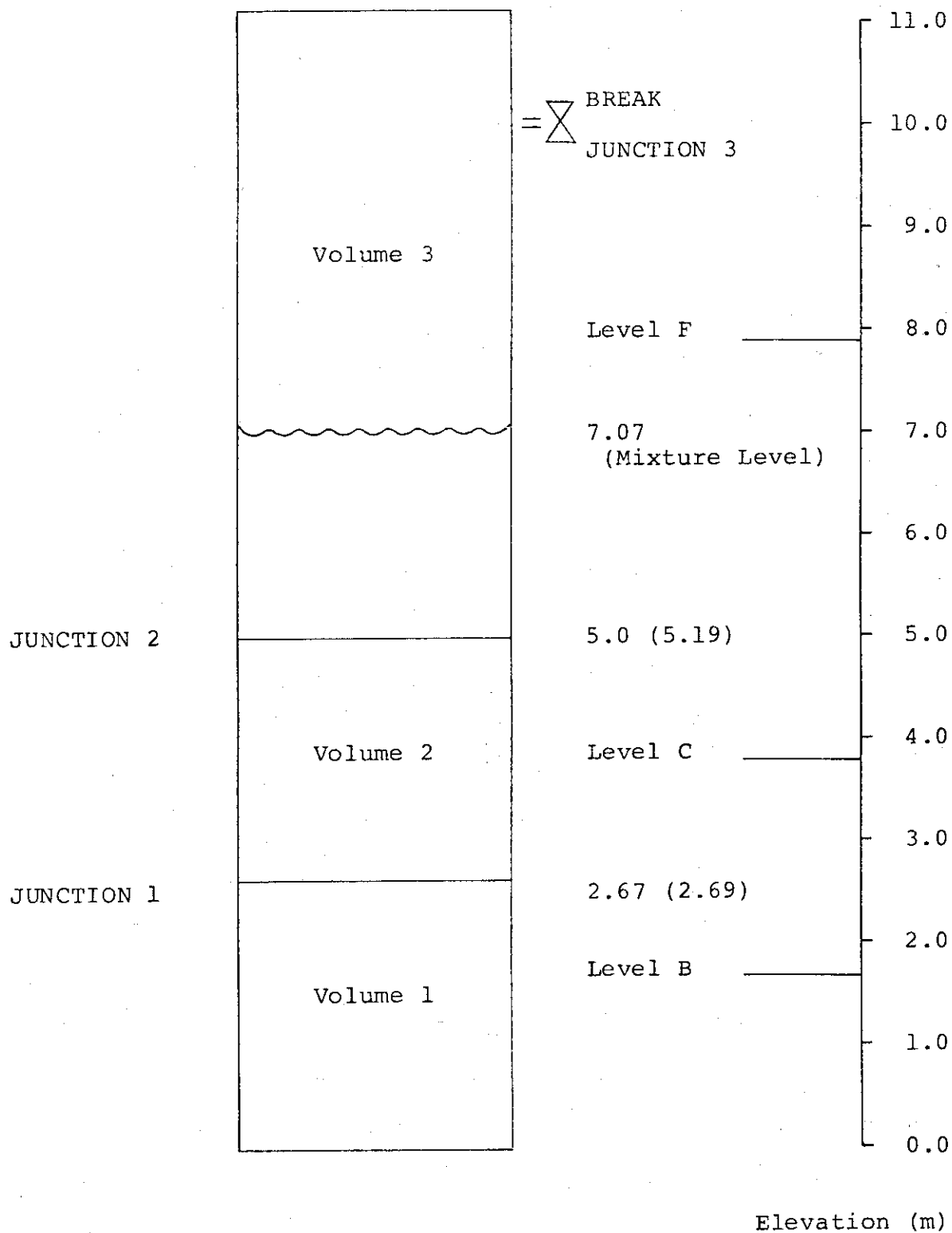


Fig. 4 Noding for ISP6
 (Bracket stands for re-analysis data)

stacked control volumes, often provide some physically unrealistic results with regard to the water level. For instance, when this model was applied in volume 2 and 3, there is a mixture level in the two control volumes at the same time. Hence, such a model is only available to the top node.

The whole movement of the free surface between the vapor and two-phase mixture in the vessel was calculated as the sum of the transient mixture level in the volume 3 plus its elevation (5.0 m or 5.19 m).

As the present calculation was performed with a very simple nodding method, the experimental measured data at the specified locations and the prediction may be consistent or not. It is difficult to obtain for the current ALARM-B1 three volume model all the required outputs related to the pressure and the temperature as a CSNI request.

When taking the results of neighboring positions, the calculational results correspond to the SWR-2R apparatus data at the following measurement positions.

PRESSURE GAUGE STATION	NODE	INITIAL CONDITIONS
PS170 BI000 (Level B)	VOLUME 1	72.369 (kg/m ²)
PS380 BI000 (Level C)	VOLUME 2	72.232 (kg/m ²)
PS780 BI180 (Level F)	VOLUME 3	72.205 (kg/m ²)
TEMPERATURE GAUGE STATION	NODE	INITIAL CONDITIONS
TS170 BI000 (Level B)	VOLUME 1	289 (°C) (282)*
TS380 BI000 (Level C)	VOLUME 2	sat. (284)*
TS780 BI180 (Level F)	VOLUME 3	sat.

Table 2 Relation between Calculated Modelling and Measured data

In the table, the pressure or temperature recorded by means of station PS170 BI000 or TS170 BI000 correspond to the predictions of the control volume 1. The mass flow rate within the vessel was initially assumed to be zero (stagnant). The liquid and vapor throughout the system were also assumed to be saturated and in equilibrium. Therefore, the non-equilibrium effect is impossible to be treated without further improvement of the current mathematical model of the ALARM-B1.

No heat transfer with the structures was taken into consideration, because the observed run time was short.

Time step sizes employed in the analysis are:

$t \leq 0.5$ (sec)	$\Delta t = 0.0001$ (sec)
$0.5 < t \leq 1.0$	$\Delta t = 0.0005$
$1.0 < t \leq 3.75$	$\Delta t = 0.001$

The principal focus in the calculation was exclusively placed on the rising rate of the interface between the steam and two-phase region, and the discharge flow rate through the exit duct, which were to some extent feasible to control by a few input parameters.

In this analysis submitted to CSNI Ad hoc group, a slight error about the geometry (elevation) was discovered. Moreover, the temperature distribution in the vessel was looked again. That is, the experimental temperature and pressure profiles showed that the liquid was initially subcooled below the water level. Hence, the temperature of the volume 1 and 2 was modified. And the volume 3 was assumed to be composed of the saturated water and vapor.

After the correction of input data, re-analysis was carried out right away on a FACOM 230-75 computer. Seeing the results, the deviation in the pressure data was somewhat reduced. Significant differences between the first and second case were not observed. Geometrical configuration modelled is as follows:

VOLUME DATA			
NO.	VOLUME (m ³)	HEIGHT (m)	ELEVATION (m)
1	1.2433 (1.2526)*	2.67 (2.69)*	0.0
2	0.5998 (0.6436)*	2.33 (2.50)*	2.67 (2.69)*
3	2.8801 (2.8016)*	6.185 (6.00)*	5.00 (5.19)*
JUNCTION DATA			
NO.	ELEVATION (m)	FLOW AREA (m ²)	
1	2.67 (2.69)*	0.2574	
2	5.00 (5.19)*	0.2574	
3	9.983 (9.96)*	0.003217	

Table 3 Control Volume and Junction Identification for ISP 6

* Numbers in bracket represent modified data used in re-analysis

5. Results and Discussions

By using the computer code ALARM-B1, are demonstrated herein the calculational results for the ISP6, including the comparisons with the Battelle experimental data. Several key parameters specified at NEA CSNI were also shown in Figs.5 to 25, compared with the measured values.

A listing of the ALARM-B1 input data described in the preceding chapter is given in Appendix 1 in MKS units.

Appendix 2 is input data of re-analysis. Appendix 3 exhibits the comparisons of the observed data with a wide variety of participants' predictions of the pressure and the temperature at the selected positions, of the mixture level in the vessel and of the mass flow rate in the discharge nozzle.⁽³⁾ (see Figs.26 to 31) In these figures, the extent of deviations around the experimental values are shown for understanding the current status of predictions using the similar models as ALARM-B1. In addition, the contents of the calculational results and their modellings of participants in different countries are shown in the Tables 4 to 5, with an attention on the difference of computer simulation models.⁽³⁾

The computer run for the ALARM-B1 was terminated at 3.75 seconds. In order to present the calculational results pursuant to the predesignated formats, the plotter routine in the ALARM-B1 source program was partly modified as shown in Appendix 4.

Some short discussion of outputs and of problems encountered are given in this section.

5.1 Pressure history

The pressure transient following a guillotine steam line break was computed here.

Of particular interest in this sample problem, was the calculated pressure behavior compared with the measured one.

The ALARM-B1 theoretical prediction of the pressure was considerably higher than the Battelle-Frankfurt experimental values during the blowdown as shown in Figs.5 to 7. This experimental depressurization rate was initially large. From these figures, the pressure differential within the vessel is considered to be quite small.

In particular, the undershooting and recovery phenomenon over the first 0.50 seconds of the transient, which are due to a time delay of a steam bubble formation in the liquid portion, could not be accounted for by using the present equilibrium model.

Judging from this bubble delay behavior, it is likely that the fluid in the vessel was initially subcooled contrary to the problem conditions of saturation. On the other hand, the calculated pressure decreased at a slow pace under the saturated conditions. The transient behavior at the pressure vessel exit and interior is conceived as follows: A high temperature and high pressure fluid flow being expelled through the vessel duct, the resulting pressure falls off slowly along the saturation curve, provided that the system fluid temperature is saturated. In reality, this thermodynamical relationship of the temperature versus pressure is apt to be invalid temporarily at the very early period of the blowdown transient,

because the propagation speed of a pressure wave equivalent to a sonic velocity is faster than the phase change within the vessel.

At this time, the liquid in the vessel becomes supersaturated at the local region together with a sharp reduction of the pressure.

In succession, a steam bubble generation occurs producing the saturated water and vapor.

As a result, a metastable supersaturated state in the vessel disappears in a short time. As can be seen in the figures, a sudden decompression caused by such an initial subcooled flow regime lasts up to 0.3 seconds from the initiation of the accident, the resulting system pressure dropping below the saturation point because of a delayed bubble nucleation, *i.e.*, a time retardation of saturated water flashing to steam.

The rate of depressurization gradually decreases by the expansion of the coolant. The departure from a supersaturated state to saturated — transition region — continued for 0.2 seconds in the figures. After recovering to the saturated point, the whole system pressure decreases smoothly with the saturation from that time on. The calculated results provide the predictions which the liquid-vapor mixture is on the saturation line, showing the gradual variations from beginning to end. The initial small oscillations result from the fluctuations through the medium. The slight increase in the pressure after reaching the two-phase mixture region was impossible to be predicted well.

Perhaps this is because the analysis models preclude the volume of the discharge nozzle. The distinguished difference

between the prediction and the experimental data becomes smaller with time and three seconds later the two is well-balanced.

In the post-case analyses, the calculational results got nearer to the measured data since the pressure drops faster than those in the previous test run. (See Figs.13 to 15) At several checkout calculations, the initial conditions with some subcoolings were given in the fluid of the volume 1 or 2 in order to approach the incipient depressurization rate in the experimental data. However, this attempt was ineffective enough to change the entire behaviors owing to the lack of the non-equilibrium model.

The pressure transient response was no different than the expected gradual change in the large. Unfortunately the first pressure drop and recovery could not be reproduced correctly.

The prediction seems to be scarcely influenced due to the change of the bubble parameters, showing that the increase in the bubble rise velocity accelerates slightly the pressure reduction at the two-phase mixture region. (See Fig.23) A useful correlation of predicting the bubble delay time will be necessary to present more exact pressure profiles in the early stages of decompression. As a few predictive methods, the experimental or theoretical formulas to compute a bubble growth is reported in the reference. (4) (9) (10) (11)

For reference, the initial pressure gradient derived from the isentropic expansion of the vapor phase was determined from the following hand calculation. Namely, using the assumption of the adiabatic law

$$P v^k = P_0 v_0^k = \text{constant} ,$$

the initial decompression rate is calculated as follows:

By differentiating the above formula,

$$\dot{P}_O = -k \frac{P_O}{V_O} \dot{V}_O = -k \frac{P_O}{V_S} (\dot{V}_S)_O = -k P_O \left(\frac{W_S}{\rho_S V_S} \right)_O$$

The maximum flow rate through the duct is

$$W_S = \sqrt{\frac{k}{R} \left(\frac{1}{k+1} \right)^{\frac{k+1}{k-1}}} A \frac{P_O}{\sqrt{T_O}}$$

Hence,
$$\dot{P}_O = -\frac{k}{V_S} \sqrt{\frac{k}{R} \left(\frac{2}{k+1} \right)^{\frac{k+1}{k-1}}} \frac{A P_O^2}{\rho_S \sqrt{T_O}}$$

From the initial state data

$$\left\{ \begin{array}{l} P_O = 72.0 \times 10^4 \text{ (kgf/m}^2\text{)} \\ A = 3.217 \times 10^{-3} \text{ (m}^2\text{)} \\ v_O = 0.0271 \text{ (m}^3\text{/kgm)} \\ V_S = 2.88 \text{ (m}^3\text{)} \\ k = 1.4 \end{array} \right.$$

$$\dot{P}_O = -k \sqrt{k \left(\frac{2}{k+1} \right)^{\frac{k+1}{k-1}}} \frac{A P_O}{(V_S)_O} \sqrt{\frac{P_O}{V_O}} \text{ (from ideal gas equation)}$$

$$= -1.4 \sqrt{1.4 \left(\frac{2}{2.4} \right)^{\frac{2.4}{0.4}}} \frac{A P_O}{(V_S)_O} \sqrt{\frac{P_O}{V_O}}$$

$$= -1.4 \sqrt{1.4 \cdot 9.8 \left(\frac{2}{2.4} \right)^6} \frac{A P_O}{(V_S)_O} \sqrt{\frac{P_O}{V_O}}$$

$$= -3.0096 \cdot \frac{72 \cdot 10^4 \cdot 3.217 \cdot 10^{-3}}{2.88} \sqrt{\frac{72 \cdot 10^4}{0.0271}}$$

$$= -33.7 \text{ (kgf/m}^2 \cdot \text{sec)}$$

On the other hand, the experimental pressure gradient is

$$-(72-67)/0.15 = -33.3 \text{ bar} = -34 \text{ (kgf/m}^2 \cdot \text{sec)}$$

A comparison of the values between the two is in the excellent concurrence.

NOMENCLATURE : P = pressure

T = temperature

v = specific volume

k = ratio of specific heats

V = volume

A = flow area at duct exit

R = universal gas constant

W = mass flow rate

Subscript "O" and "S" mean the initial time and steam space, respectively. Dot means differential with respect to time.

5.2 Temperature history

The fluid temperature profiles were relatively fair between the calculated and measured values, although the former is about 6~7 °C higher than the latter at the initial stages. (see Figs. 8 to 10) This small discrepancy might be caused by the inconsistency of the reported experimental conditions. The experimental was certainly below the saturation temperature during the first 0.50 seconds. Due to some subcooling in the liquid portion, it resulted in a rapid decrease in the pressure as already stated.

The temperature recovers to the saturation point 0.50 seconds later, then remaining there. On the other hand, the calculated temperature was saturated throughout the blowdown.

Since the initial temperature distributions have possessed the uncertainty considerably, more exact temperature profiles should be given as the recommendation to this experiment.

Re-calculations had bettered the temperature more or less except in node 3. (see Figs. 16 to 18)

5.3 Liquid level history

The rise of the interface between the initial steam and the saturated two-phase mixture was predicted in Fig. 11.

As already indicated in the pressure behaviors, an identical difference attributable to the thermo-dynamical non-equilibrium feature was also observed with reference to this parameter. It is obvious that the experimentally measured water level in the vessel during the early time of the blowdown transient did not significantly swell owing to the evaporation delay and incompressibility. From this fact, it was confirmed that the water level rising and pressure recovery are so closely linked. After about 0.3 seconds, the steam-water mixture level increases almost linearly from the initial 7.07 m together with growth of steam bubbles. The rising velocity of the calculated liquid level is 1.133 (m/sec) while the one of the measured exhibits 1.344 (m/sec). At 2.55 seconds the calculated water level reaches the height of the discharge line.

A slip ratio between the phase, which is not incorporated in the ALARM-B1 homogeneous model, (slip ratio is 1.0 due to equal fluid velocity) would exert influence on the water level in the transient like a bubble-rise velocity.

In the experimental data, it is noted that there was a

small discrepancy between the time (about 2.5 seconds) when the mixture front reaches the outlet nozzle (G) and the time (about 2.2 seconds) when the effluent flow increases abruptly.

The latter is slightly fast compared with the former. It is presumably due to the fact that entrained droplet was present above the free surface and that liquid flowed through the blow-down nozzle.

The calculational model in ALARM-B1 does not treat such entrainment phenomena, therefore there was no significant difference between these prediction times in contrast with observed in the experimental data. That is, an increase in the liquid level to the height of the discharge line coincides with a step change in the mass flow rate. The saturated mixture in ALARM-B1 predictions begins to carry over into the steam line inlet at 2.55 seconds. The calculation of the liquid level in the control volume strongly depends on the bubble rise parameters given by constant input data during the blowdown. (See Fig.24)

In practice, a bubble rising in the vessel would be affected by the degree of some subcoolings and the amount or location of subcooled water. Thus, the selection of bubble parameters was difficult and determined by rule of thumb criteria derived from the previous experience. (7) (11) (13)

Aside from this analytical method, for instance, the Wilson's model representing the bubble velocity as a function of mixture void fraction would help handling more exact bubbling phenomena. (12)

In general, a higher bubble rise velocity results in the lower liquid level swelling. The reason is; By the increase of this velocity or slip ratio, steam bubbles in the liquid

becomes low. Hence, the expansion of the mixture, i.e., flooding rate is suppressed down. Since the calculation was initiated at the saturation condition, flashing occurs immediately in the vessel. Accordingly, it reduces to an instantaneous rising in the mixture level as well as a slower continuous decrease in the pressure. In this way void formation due to flashing is the only contribution to water level rise. Throughout some check runs, an optimum bubble rise velocity was 3 ft. (Fig.19, Fig.24)

Additionally it should be noted that the water level also depends on even the Moody's coefficient, which was set to 0.75 at the current analyses. When adopting a small discharge factor, a lower decompression rate results in a reduced rate of flashing within the vessel and a reduced rate of level rising.

5.4 Discharge mass flow rate history

A discharge flow transient was divided into three phases: the vapor flow, the transition from the vapor to saturated two-phase mixture flow and the subsequent mixture flow.

As illustrated in Fig.12, a comparison of the predicted effluent flow rate and the experimentally measured data at the exit duct is quite good through the transient within the 10~15 % instrument error bands, except for the first short period of the blowdown (0~0.05 seconds) and for the two-phase mixture region. The non-equilibrium effect was not, in fact, identified in the behavior of the discharge flow. The calculated result with a Moody's contraction coefficient of 0.75 was in excellent agreement with the observed value.

Immediately after the rupture, the steam flow rate increases

to the maximum value permitted by choking at the outlet junction. This break has made a large pressure drop across the outlet because of the high vapor flow rate. The ALARM-B1 was not capable of predicting the first peak (about 36~7 kg/sec) shown in the experimental curve.

Through the orifice, the steam discharge lasts till 2.55 seconds, thereafter carry-overed two-phase mixture flow does.

When the water level increases to as far as the elevation of the discharge nozzle G, the blowdown flow rate ascends suddenly due to the transition from the vapor to the steam-water mixture. This change involves a reduction of the flow quality at the exit plane. (see Fig.21) By outflowing of the steam flow, a moisture begins to carry-over into the steam dome.

The transition from the steam to mixture gives a step change in the ALARM-B1 model. On the other hand, this characteristic in the experimental occurs over a period of approximately 0.2 seconds.

A marked discrepancy between the two does result from the inability of this code to simulate the entrainment phenomenon. This change from the steam to the mixture flow has a slight effect of reducing the vessel depressurization rate as reflected by the small variation in slope of Fig.7.

During the discharge of the mixture flow, a peculiar behavior in the ALARM-B1 is due to the partial presence of a bubbly-flow produced by a decompression in the intervals of steam-water mixture flow. Transient two-phase flow predicts as if its flow pattern is of slug flow. As shown in the outflowing of the mixture, the amount of effluent two-phase flow agrees

with that of the measured on the average.

Fig.22 shows the mass inventory transient in the vessel. As already stated, lower bubble rise velocity results in smaller mass hold up.

The post calculations almost agrees with the first one. When the bubble-slope parameter decreases, the resulting two-phase discharge flow increased.(see Fig.25)

6. Summary

The Standard Problem NO.6 based on a high pressure and a high enthalpy blowdown test SWR-2R was analyzed by the ALARM-B1 code.

Comparative studies were made with the theory and experimental data. The predictions indicated that homogeneous equilibrium models applied to the initial fluid behavior in the vessel were inadequate to explain the measured pressure or liquid level.

However, by and large, this test runs to make certain the analytical models of the ALARM-B1 were apparently successful with a few exceptional behaviors arising from the non-equilibrium. Namely, the current calculational work was useful for the purpose of checking the program and obtaining more experiences for its use. The measured rapid depressurization, consequent recovery and delayed liquid level rise appear to be associated with the thermal non-equilibrium effects accompanied by the bubble-nucleation delay.

These parameters showed relatively poor agreements between the calculational and measured values. The large pressure waves occurred in the early stages of the blowdown might cause a damage to the pressure vessel owing to the great thrust force. Accordingly, the prediction of such pressure waves seems to be important to the safety assessment of the plant in some cases.

In the present analysis, the initial temperature distribution is especially important because the transient system states, thereby, were determined. In the experiment, there were inconsistent differences between the reported initial temperature

distribution in the vessel and the experimentally measured temperature distribution. Probably, the desired temperature could not have established in the beginning. Full detailed temperature characteristics should be given. To minimize the deviations between the predictions and the experimental results, the adjustable parameters to approach the measured data were only limited to the bubble slope data and the discharge coefficient.

From the parameter studies performed, the water level rise was greatly influenced by the variations in the bubble rise velocity.

An increase in the value of this parameter caused a delay in the liquid level swelling. An increase in the bubble density gradient caused a decrease in the maximum value of the discharge mass flow.

On checking the experimental results, new aspects such as the liquid superheat, bubble nucleation delay or the relaxation time proved to be necessary to trace the phenomenon more realistically.

Nevertheless the first part of system behavior with the principal attention on non-equilibrium might be, in a sense, unnecessary to concentrate more energies from the standpoint of the long term blowdown analysis, because the system performance for the saturation blowdown calculations was adequate in the large by using the current equilibrium code. In that case, needless to say, it is of vital importance to keep in mind the assumptions or the limitations lying behind its use.

Speaking of time step sizes used, they did not lead to numerical instability throughout this calculation.

7. Concluding Remarks

On the whole, the comparison of the theoretical predictions and the measured data for the ISP6 did not show the satisfactory agreements. The main differences would be attributable to the deficiency of the non-equilibrium model in the computer code. The following conclusions can be drawn from this verification run.

- (1) The discharge flow model in the ALARM-B1 was reasonably good compared with the measured data. The Moody's model for this critical flow with a contraction coefficient of 0.75 was sufficient in the steam region of the transient, but predicted a bit highly in the two-phase mixture flow region.
- (2) The use of a bubble-rise model to predict the swelling of the liquid level was tracked adequately within the capability of the equilibrium code. Although the measured gradient was somewhat steeper than the computed one, the agreement related to the time reaching the top nozzle is considered to be good. An introduction of the bubble growth mechanism within the vessel would play a central role in the analysis of the non-equilibrium phenomenon.
- (3) A rapid decompression history attributed to the non-equilibrium properties could not be reproduced well. It shows that the saturated two-phase fluid assumed in the vessel was not, in fact, initially at the equilibrium due to the local subcooled liquid portion. Starting with the saturation in the ALARM-B1 analysis, did produce a slow continuous decrease in the pressure. As well, the consequent recovery was not predicted within restrictions in

this code.

As concluded, it might be highly expected that further examinations of the analytical models such as non-equilibrium phase change, entrainment, slip velocity, or bubble growth mechanism would contribute to give better results.

Acknowledgement

Much appreciation is expressed to Mr. K. Sato, the chief of Reactor Safety Code Development Laboratory, and to Mr. M. Akimoto for their useful suggestions in writing this paper.

References

1. B. Hölzer, T. Kanzleiter, F. Steinhoff : Specification of OECD STANDARD PROBLEM NO.6, Determination of Water Level and Phase Separation Effects During the Initial Blowdown Phase, Battelle Institute, Frankfurt, Feb., 1977, (Drawings, No.R61 797-2703, R61 797-14036)
2. M. Akimoto, ALARM-B1 : A Computer Program for Boiling Water Reactor Blowdown Analysis, JAERI-M 6968, Mar., 1977
3. W. Winkler, CSNI Report NO.30 Comparison Report on OECD-CSNT STANDARD PROBLEM NO.6, Aug., 1978
4. A.R. Edwards : Conduction Controlled Flashing of a Fluid and the Prediction of Critical Flow Rates in a One-dimensional System, AHSB(S)-R-147, 1968
5. Gordon C.K. Yeh, N. Suber : On the Problem of Liquid Entrainment, ANL-6244, Sep., 1960
6. A.H. Shapiro : The Dynamics and Thermo-Dynamics of Compressible Fluid Flow, vol.1
7. K.V. Moore, W.H. Rettig : Relap-4 A Computer Program for Transient Thermal Hydranlic Analysis, ANCR-1127, Dec., 1973
8. F.J. Moody : Maximum Flow Rate of a Single Component, Two-phase Mixture, J. of Heat Transfer, Trans. ASME, 87, NO.1, 1965
9. D.L. Hunt : The effect of Delayed Bubble Growth on the Depressurisation of Vessels Containing High Temperature Water, AHSB(S) R.189, Nov., 1970
10. O.C. Jones, P. Saha : Non-equilibrium Aspects of Water Reactor Safety, BNL-NUREG-23143, Jul., 1977

11. K.V. Moore, R.P. Rose : Application of a Lumped Parameter Bubble Rise Model to Coolant Blowdown Analysis, Trans. Am. Nucl. Soc., 9, 2, 1966
12. J.F. Wilson, et al : The Velocity of Rising Steam in a Bubbling Two-phase Mixture, ANS/TRANS/, 5, 1962
13. M. Akimoto, F. Araya, S. Sasaki, K. Sato, ALARM-Pl : A Computer Program for Pressurized Water Reactor Blowdown Analysis, JAERI-M 8004, Dec., 1978

Table 5 Important Features of Simulation Models Using

Equilibrium Codes

Country	Australia	Germany	Italy	Italy	Japan
Code	NAIAD (with vessel model)	BRUCH-S	RELAP-UK	RELAP4/MOD5 *	ALARM1-BL
discharge model	HEM	Moody	Moody	Moody	Moody
discharge coefficient	contraction pressure loss coefficient $f \frac{L}{D} = 0.1$	1.0	1.0	0.7	0.75
number of nodes (liquid/steam/discharge nozzle)	$\frac{1}{2} / \frac{1}{2} / 11$	$\frac{7}{2} / \frac{1}{2} / 0$	6	1/1/0	$\frac{1}{2} / \frac{1}{2} / 0$
bubble rise velocity ($\frac{m}{s}$)	0.9	according to Wilson, up to 0.9	0.91	0.15	0.03
bubble rise gradient parameter	0	quality gradient 3	0.8	0	0.7
slip	no	no	yes	yes	
number of heat slabs		none	-		
initial liquid subcooling; maximum temperature difference (K)	yes, 2.2	no	no	yes, 4.4	
time step size Δt (sec)	$1 \cdot 10^{-4} - 1 \cdot 10^{-2}$	varying, $5 \cdot 10^{-1} - 3 \cdot 10^{-2}$		$0 < t < 0.5: 0.0001 < \Delta t < 0.01$ $0.5 < t < 3.0: 0.0005 < \Delta t < 0.05$	$0 < t < 0.5: \Delta t = 0.0001$ $0.5 < t < 1.0: \Delta t = 0.0005$ $1.0 < t < 3.0: \Delta t = 0.001$

f = Fanning friction factor
t = problem time (sec)
D = diameter
L = length

* calculations submitted after deadline to the workshop on CSNI Standard Problems at Carching, April 11-14, 1978

Table 5 (cont.): Important, features of simulation models using equilibrium codes

Country	Sweden	Switzerland	United Kingdom	United Kingdom	United States	France
Code	RELAP4/MOD3 (95) (with liquid level modification)	RELAP4/MOD2	RELAP-UK MKIII	RELAP4/MOD3 (WREM)	RELAR4/MOD5 (2)	RELAP4/MOD5
discharge model		HEM	MEM	Moody	HEM	Moody
discharge coefficient		1.0	0.7	1.0	0.67	0.8
number of nodes (liquid/steam/discharge nozzle)	4/1/0	6/1/0	$\frac{1}{2} / \frac{1}{2} / 1$	4/1/1	6/2/1	5/1/0
bubble rise velocity ($\frac{m}{s}$)	0.91	0.91	0	0.91	0.15	0.30
bubble rise gradient parameter	1.0	0.8	0	0.8	0	0.8
slip		no			yes	yes
number of heat slabs				5	none	none
initial liquid subcooling maximum temperature difference (K)	yes, 6.7	yes, 3.0			yes, 6.8	
time step size Δt (sec)	$0 < \underline{t} < 0.05$: $\Delta \underline{t} = 0.00068$ $0.05 < \underline{t} < 0.5$: $\Delta \underline{t} = 0.00197$ $0.5 < \underline{t} < 3.0$: $\Delta \underline{t} = 0.0098$	$0 < \underline{t} < 0.04$: $10^{-3} > \Delta \underline{t} > 10^{-4}$ $0.04 < \underline{t} < 1.6$: $10^{-2} > \Delta \underline{t} > 10^{-3}$ $1.6 < \underline{t} < 3.0$: $10^{-2} > \Delta \underline{t} > 10^{-4}$	$0 < \underline{t} < 0.5$: $0.01 > \Delta \underline{t} > 0.0001$ $0.5 < \underline{t} < 3.0$: $0.05 > \Delta \underline{t} > 0.0005$	$0 < \underline{t} < 0.5$: $\Delta \underline{t} < 0.0005$ $0.5 < \underline{t} < 2.1$: $\Delta \underline{t} < 0.001$ $2.1 < \underline{t} < 2.6$: $\Delta \underline{t} < 0.01$ $2.6 < \underline{t} < 5.0$: $\Delta \underline{t} < 0.0005$	$\underline{t} < 0.1$: $0.0001 < \Delta \underline{t} < 0.001$ $0.1 < \underline{t} < 4$: $0.001 < \Delta \underline{t} < 0.005$	

\underline{t} = problem time (sec) * calculations submitted after deadline to the workshop on CSNI LOCA Standard Problems at Carching, April 11-14, 1978 ** post calculation

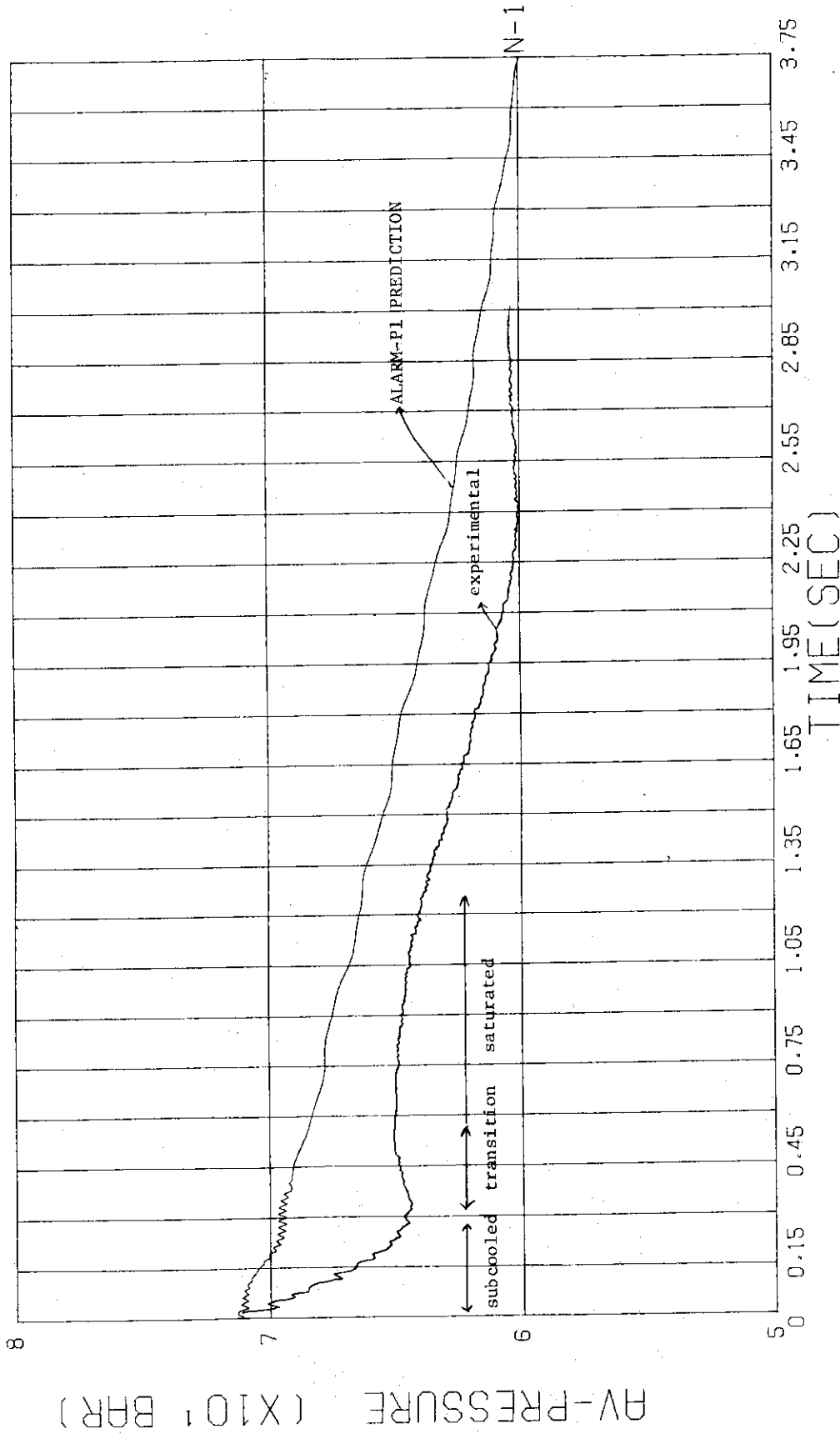


Fig. 5 Pressure in the Vessel at Level B

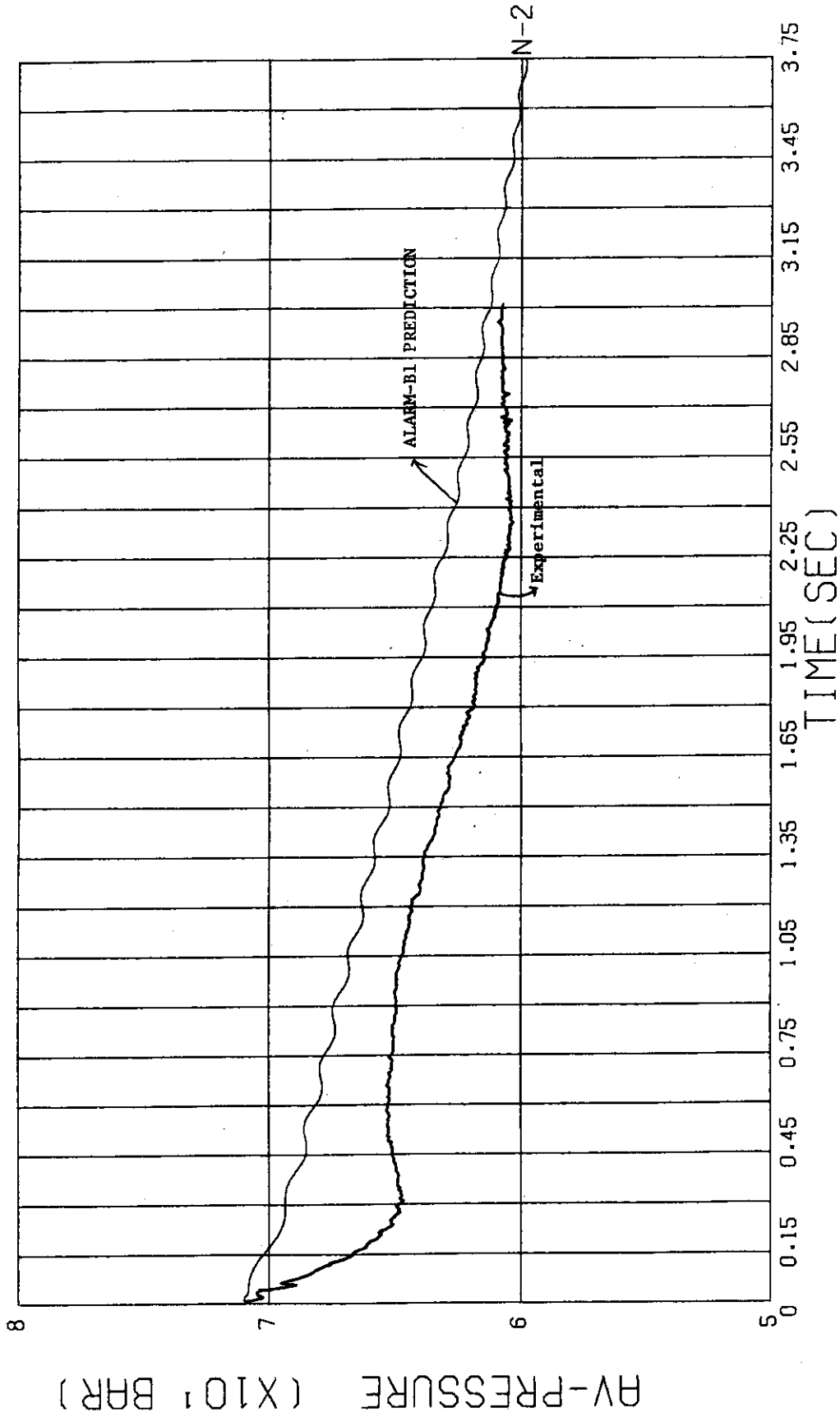


Fig. 6 Pressure in the Vessel at Level C

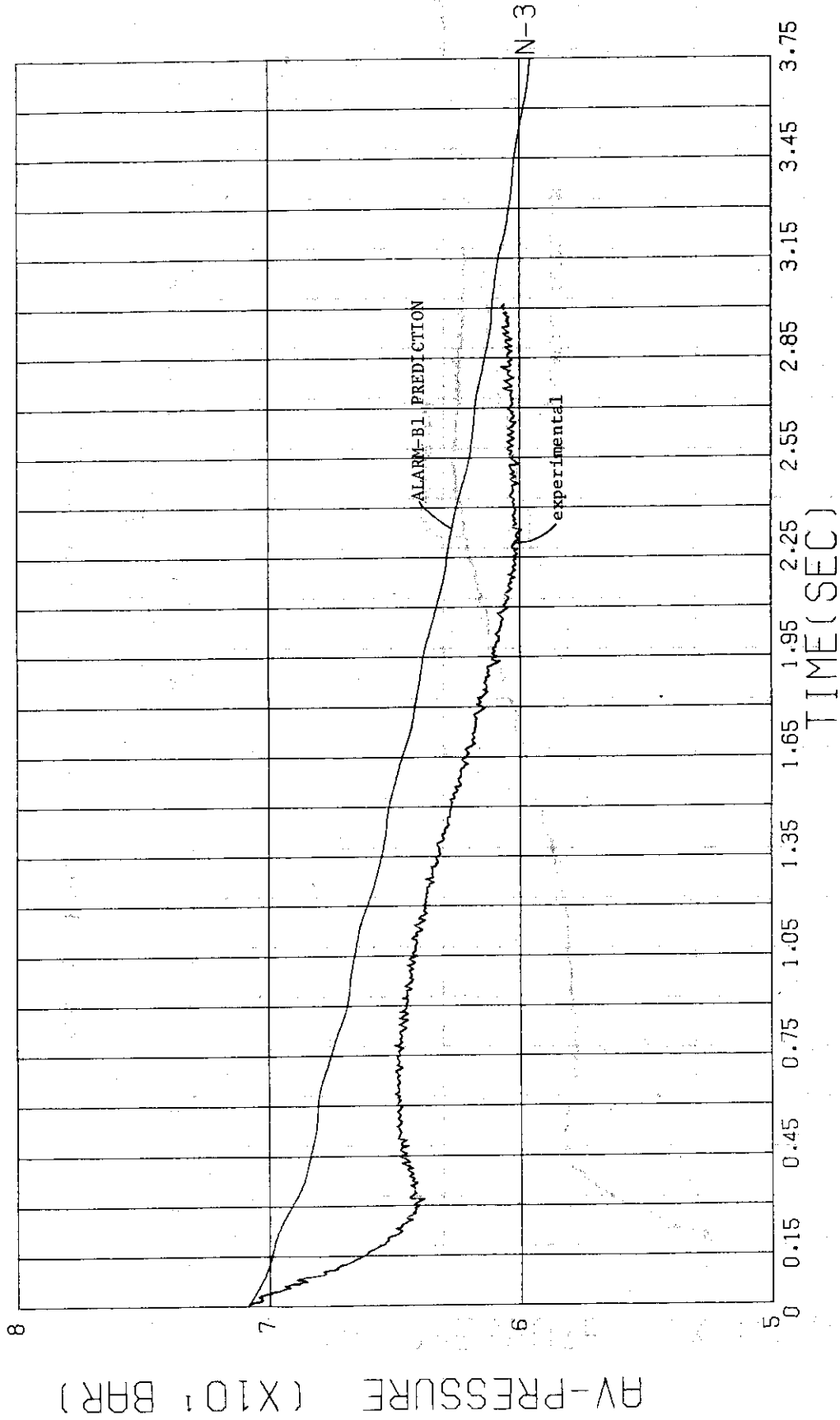


Fig. 7 Pressure in the Vessel at Level F

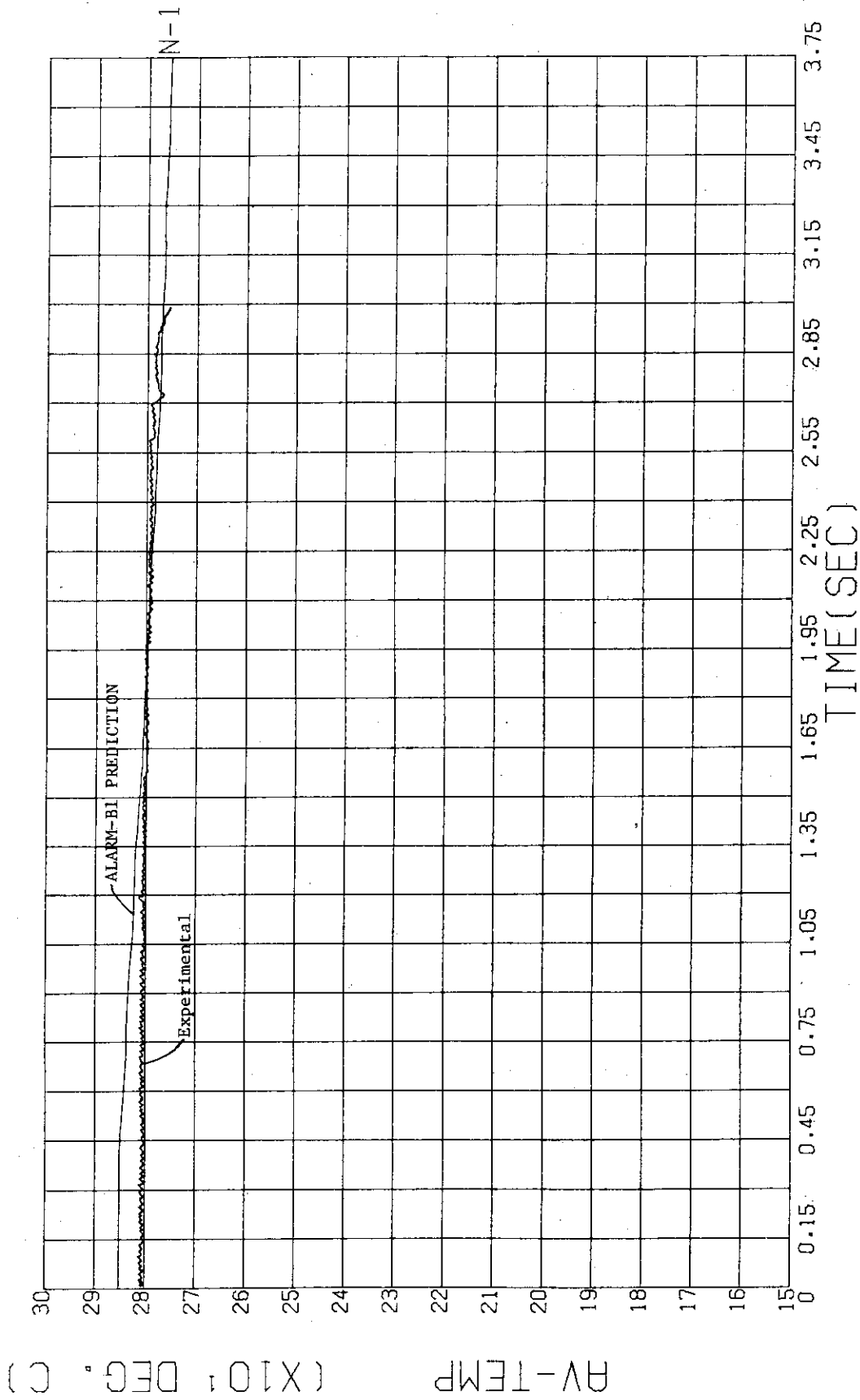


Fig. 8 Temperature in the Vessel at Level B.

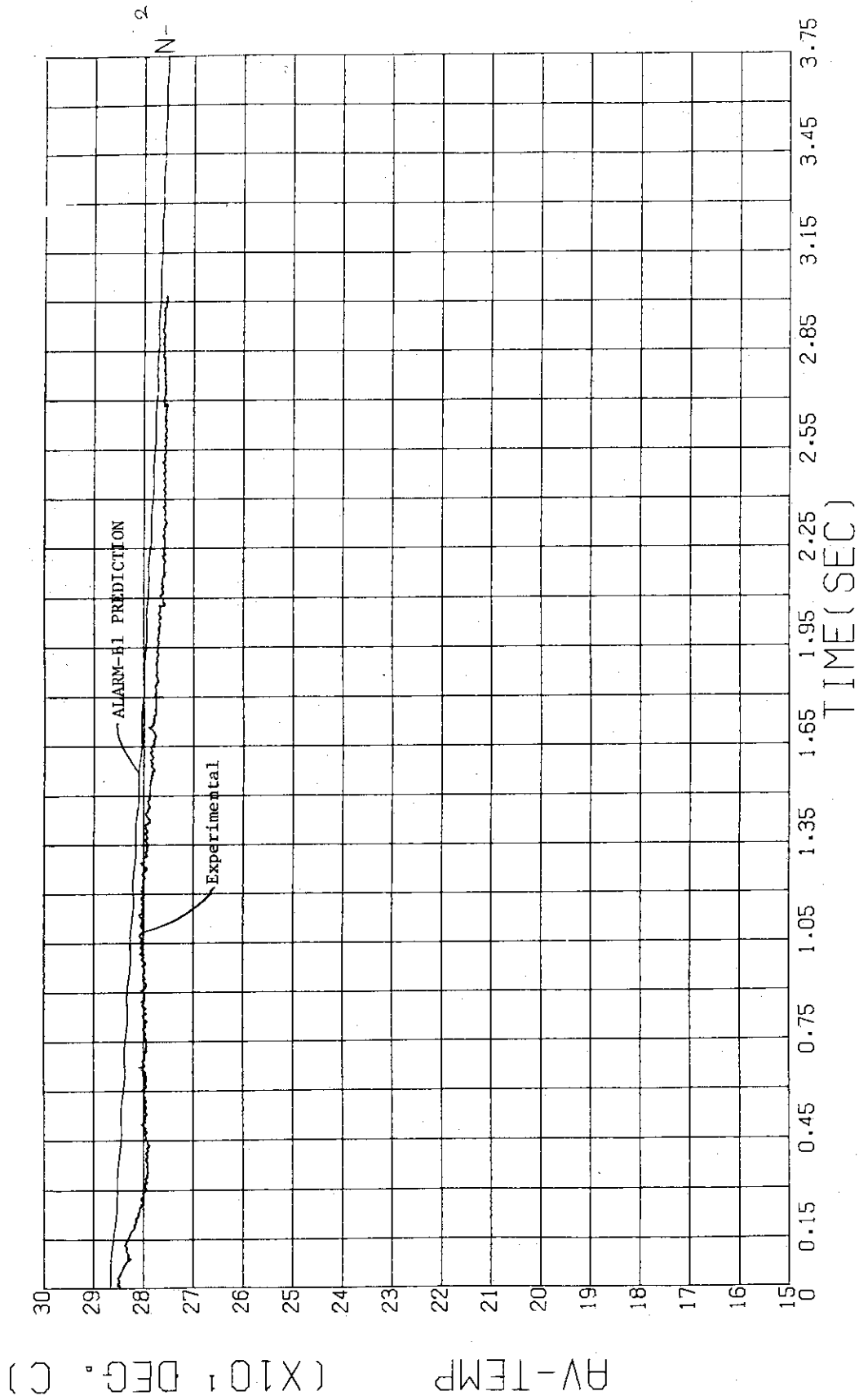


Fig. 9 Temperature in the vessel at Level C

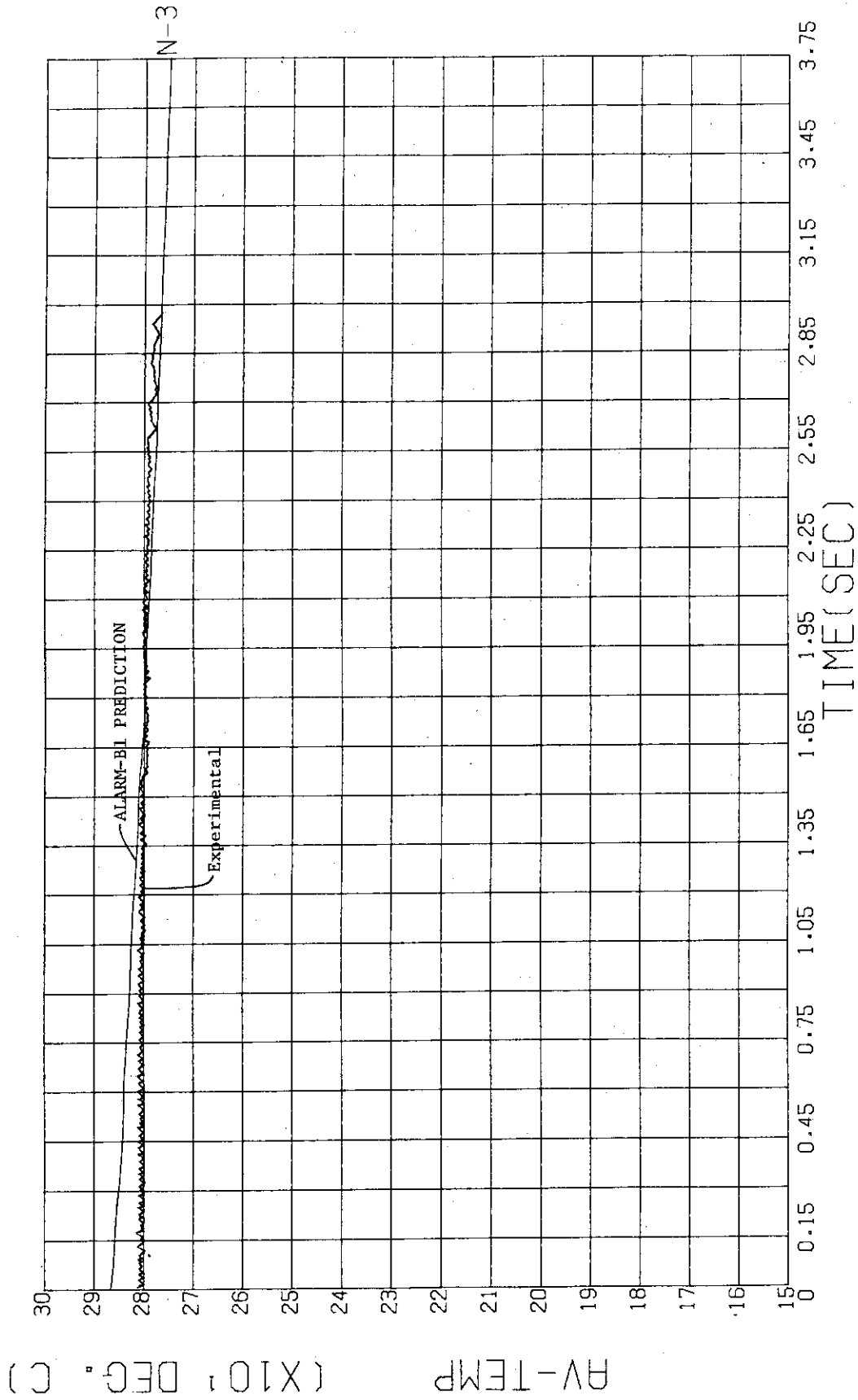


Fig.10 Temperature in the Vessel at Level F

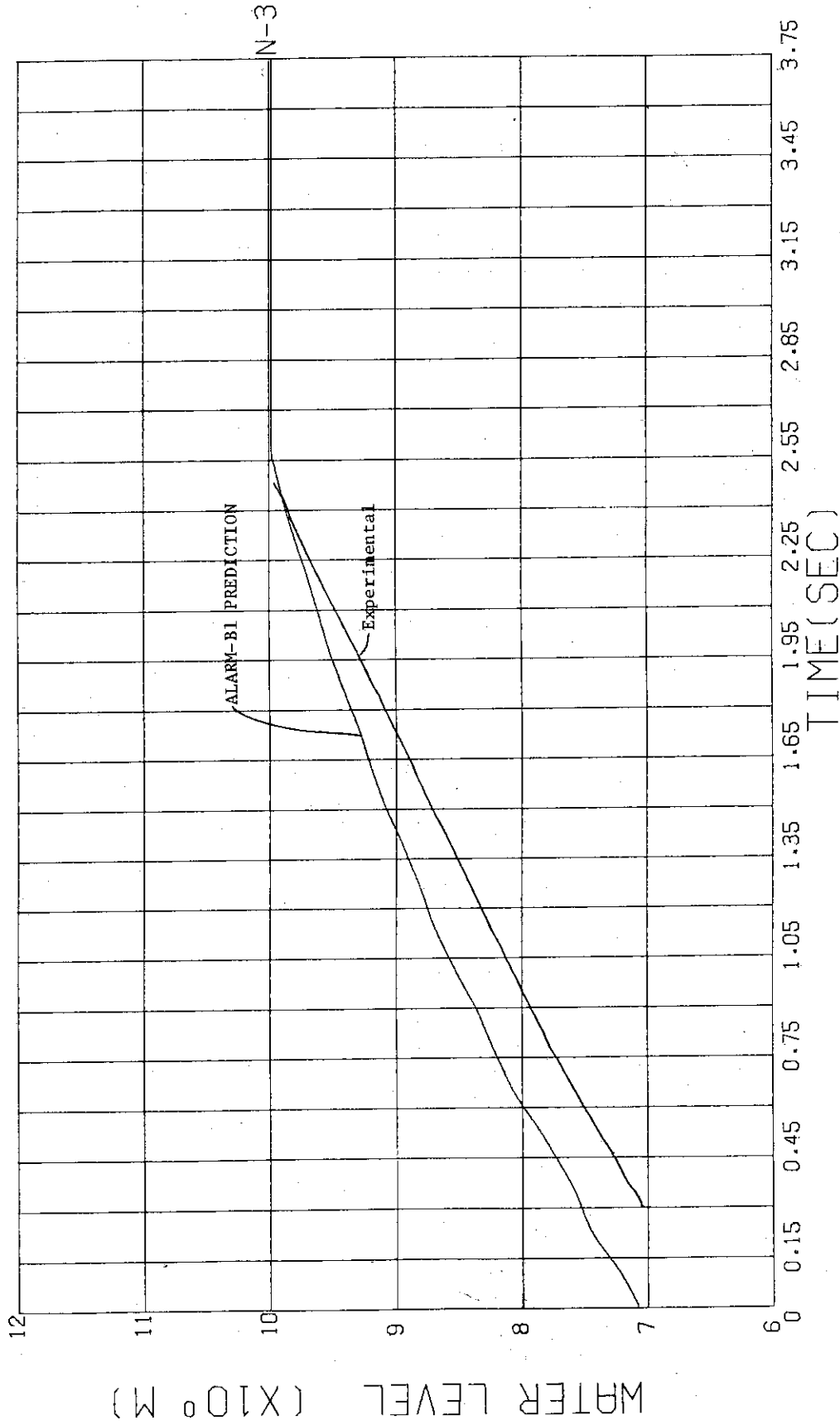


Fig.11 Liquid Level in the Vessel

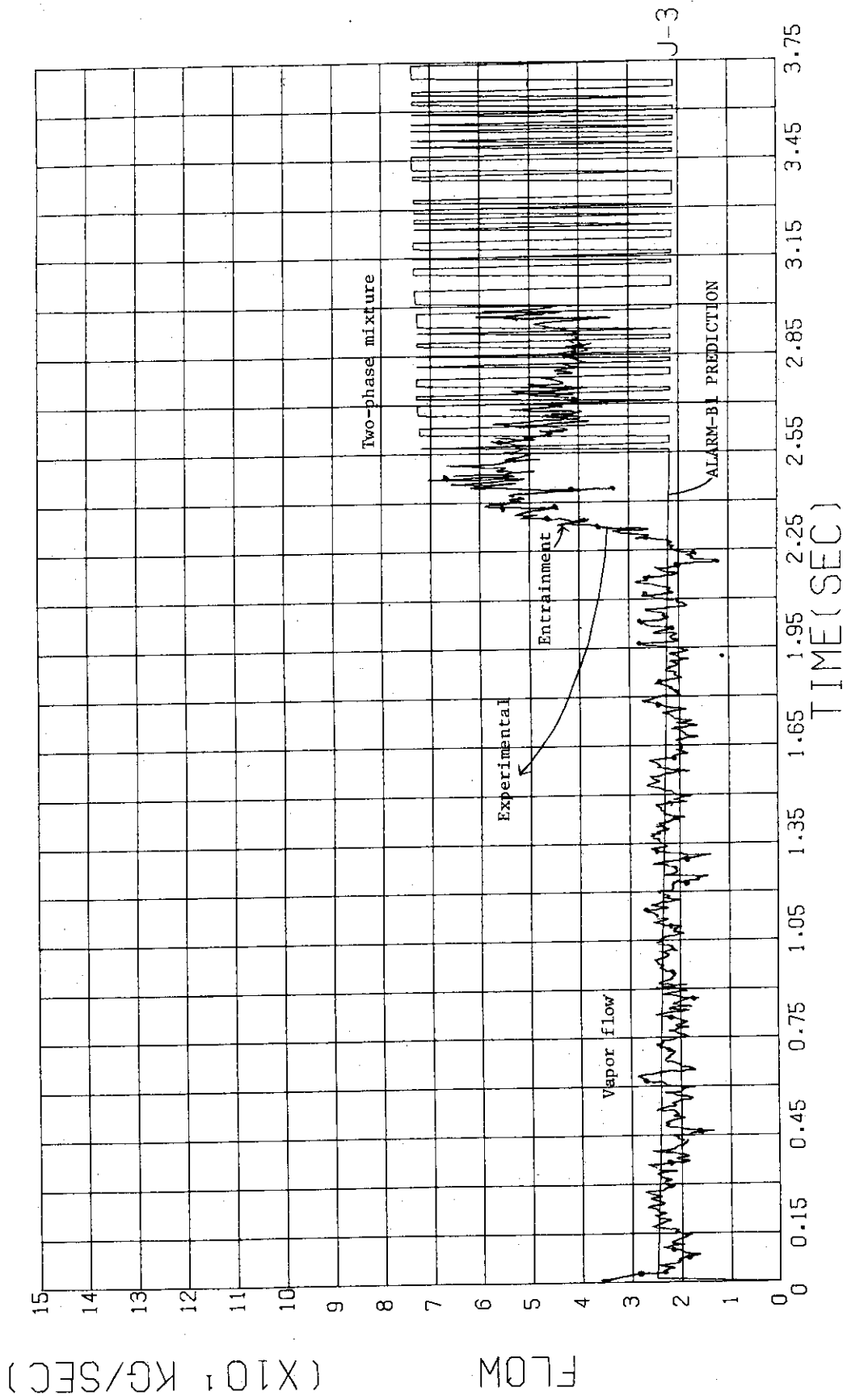


Fig.12 Discharge Mass Flow Rate

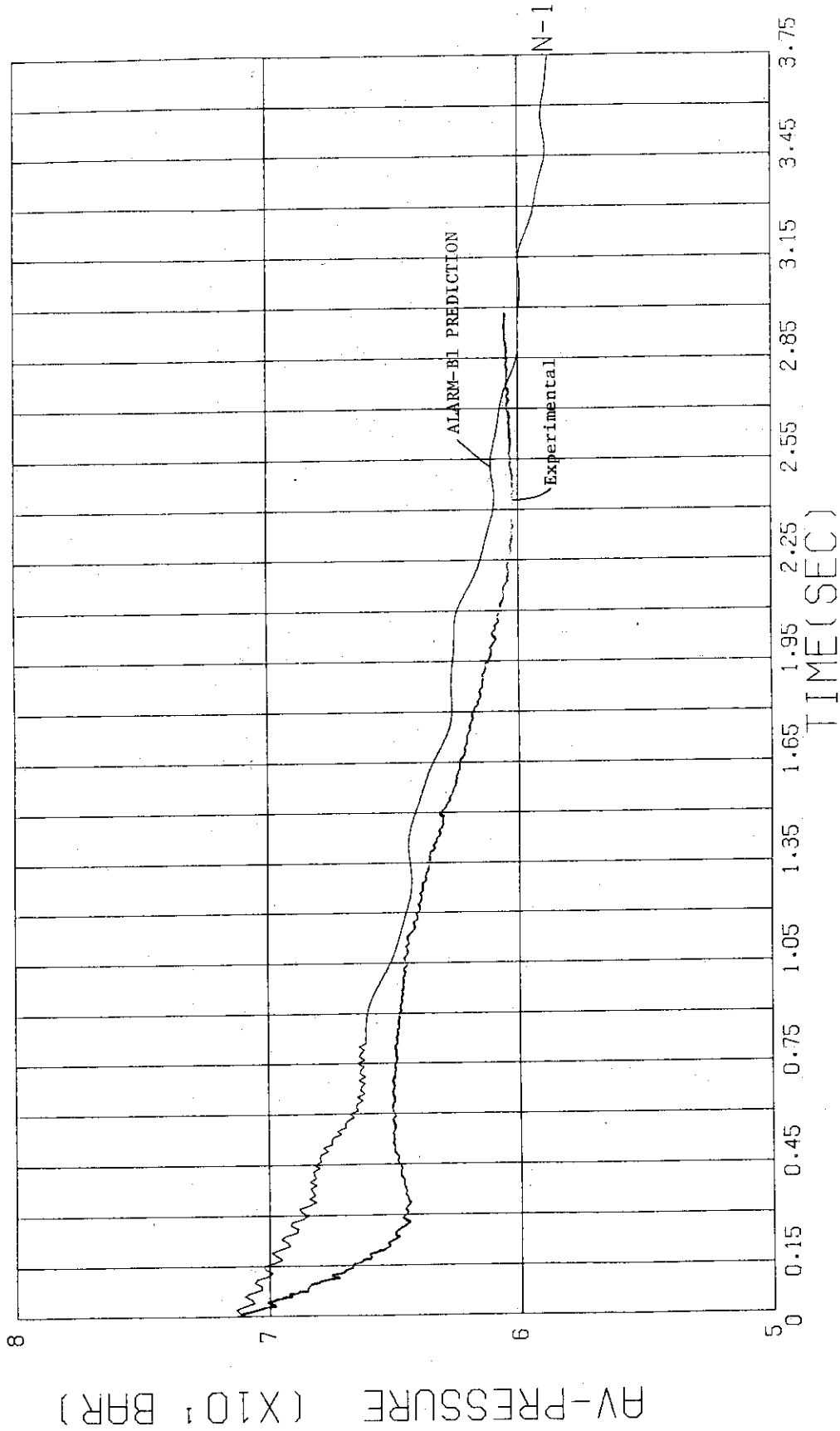


Fig.13 Pressure in the Vessel at Level B (Re-analysis)

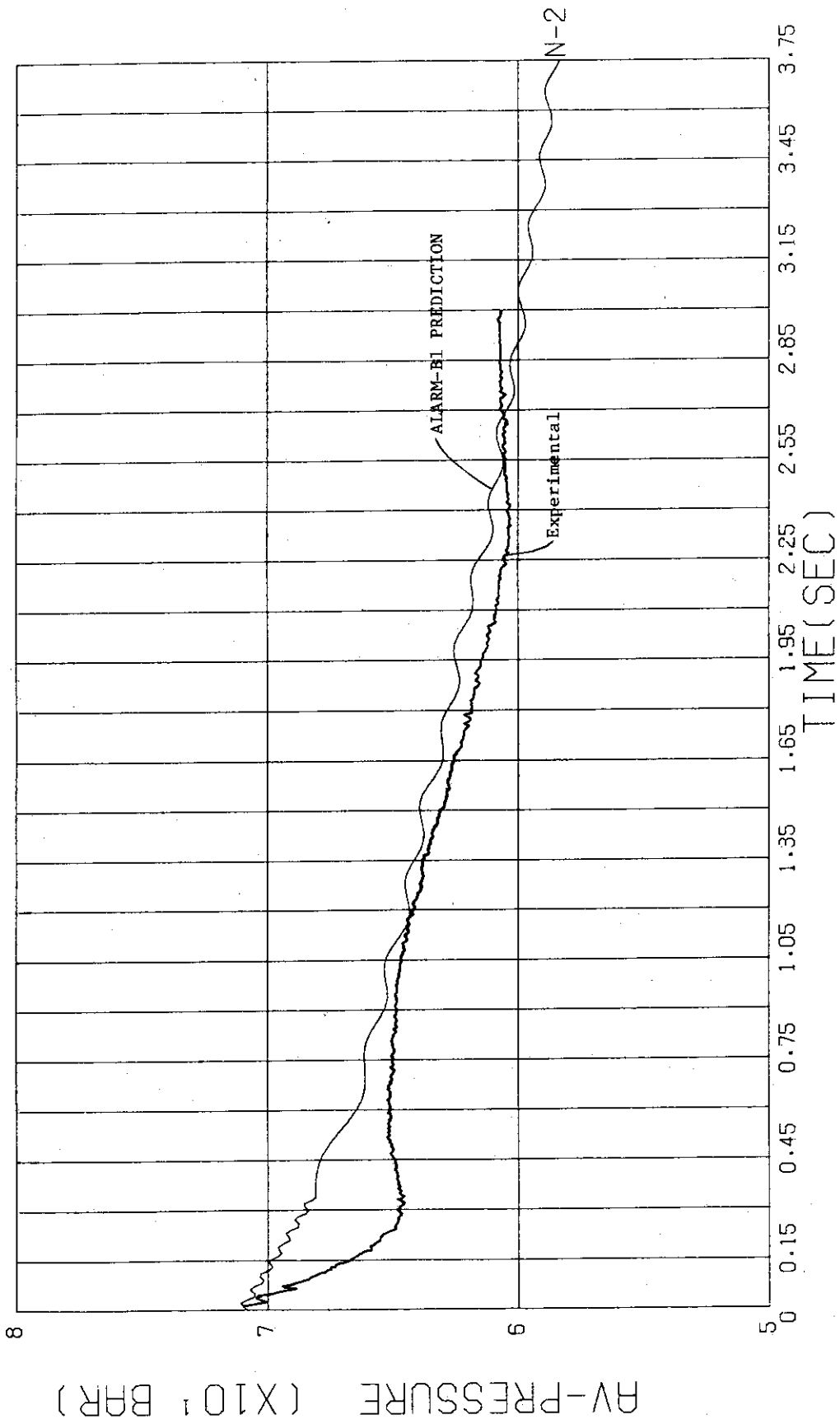


Fig.14 Pressure in the Vessel at Level C (Re-analysis)

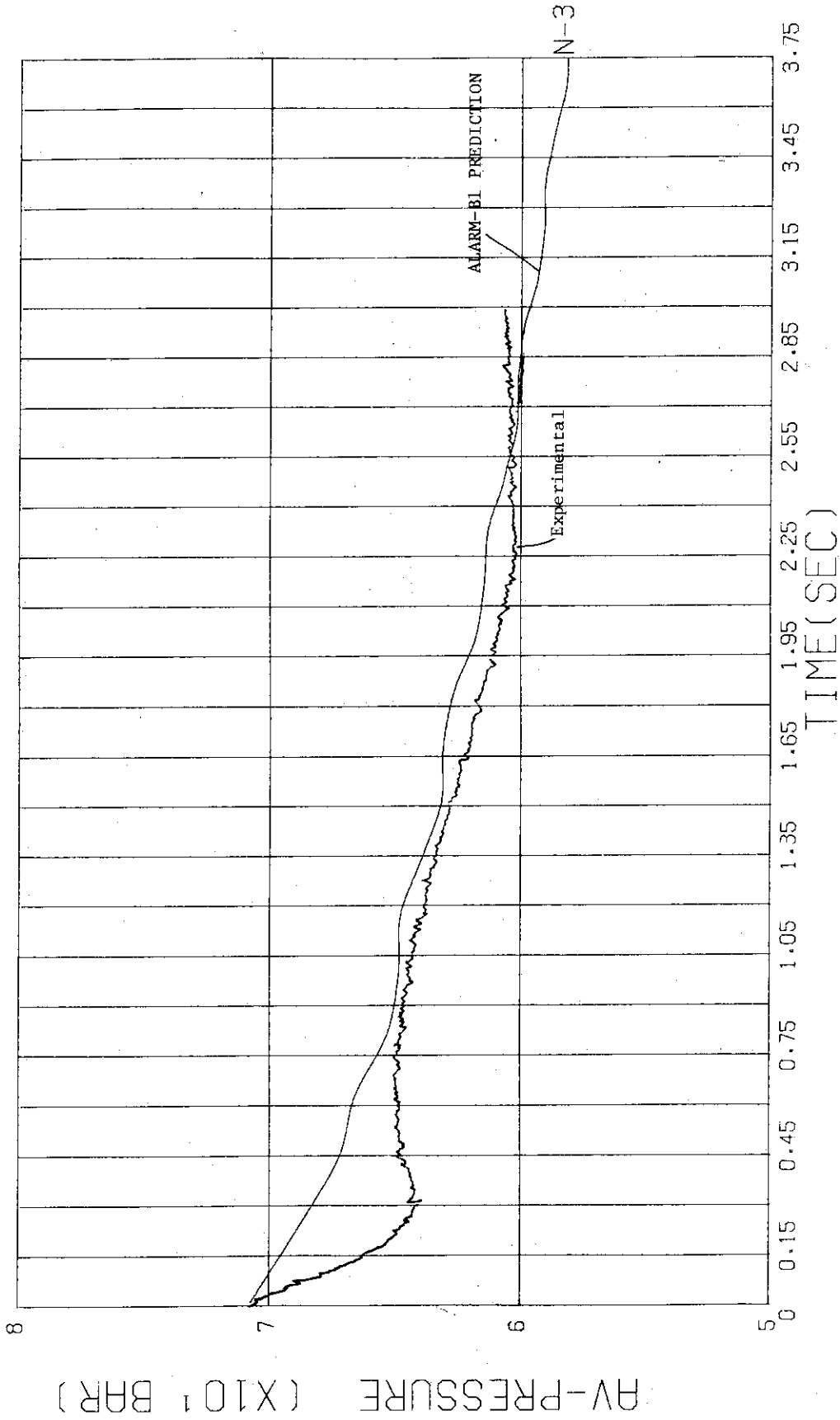


Fig.15 Pressure in the Vessel at Level F (Re-analysis)

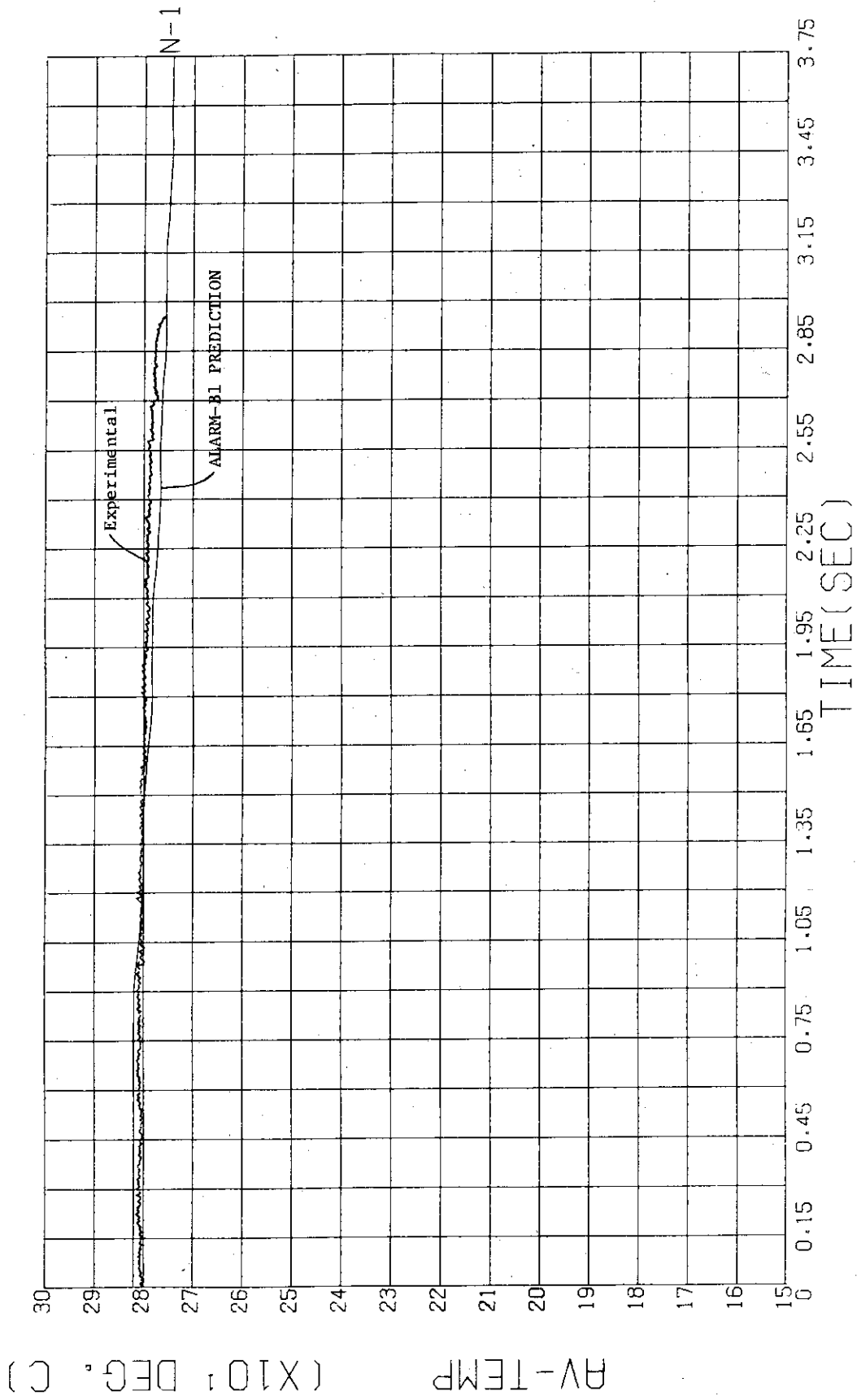


Fig.16 Temperature in the vessel at Level B (Re-analysis)

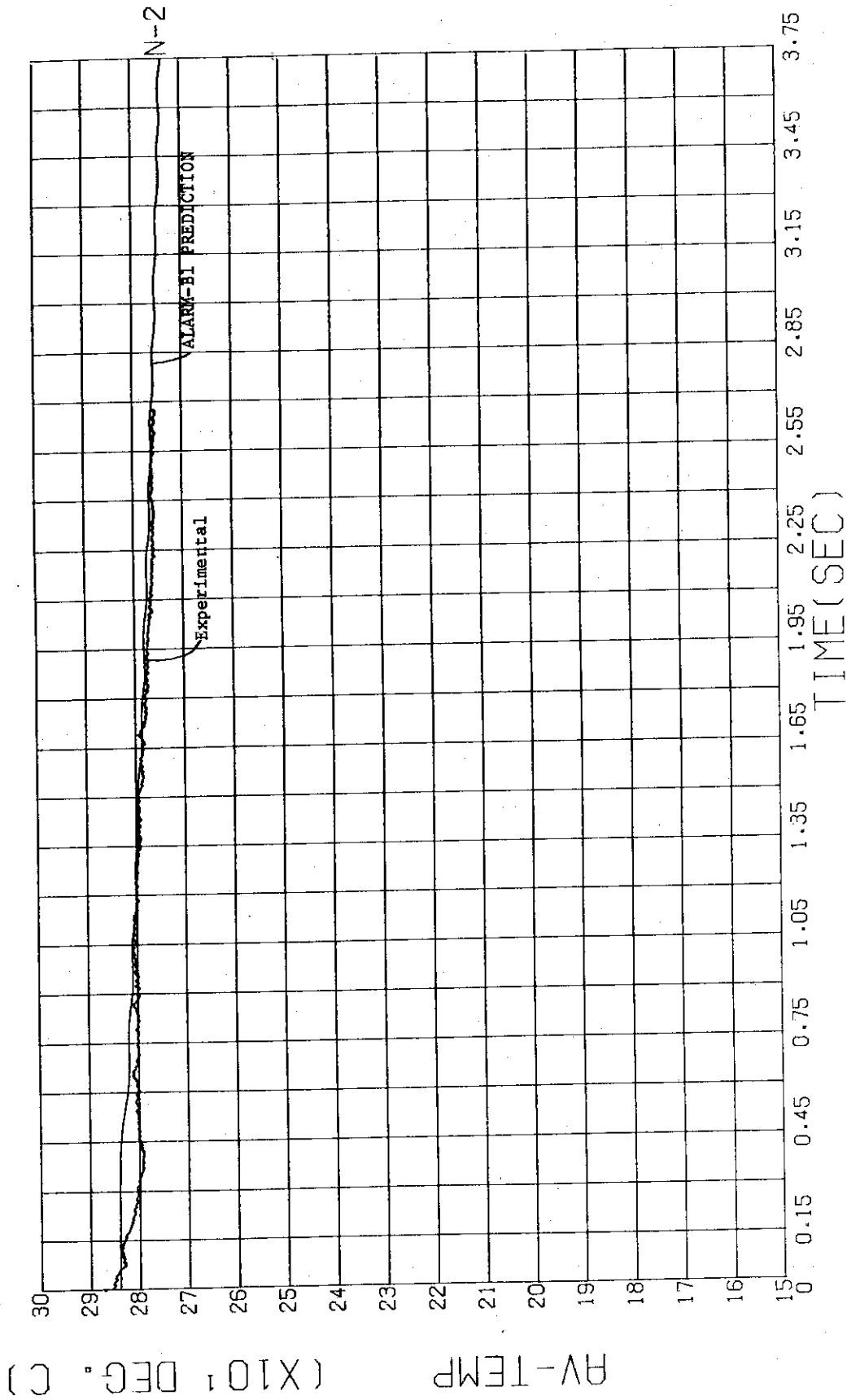


Fig.17 Temperature in the Vessel at Level C (Re-analysis)

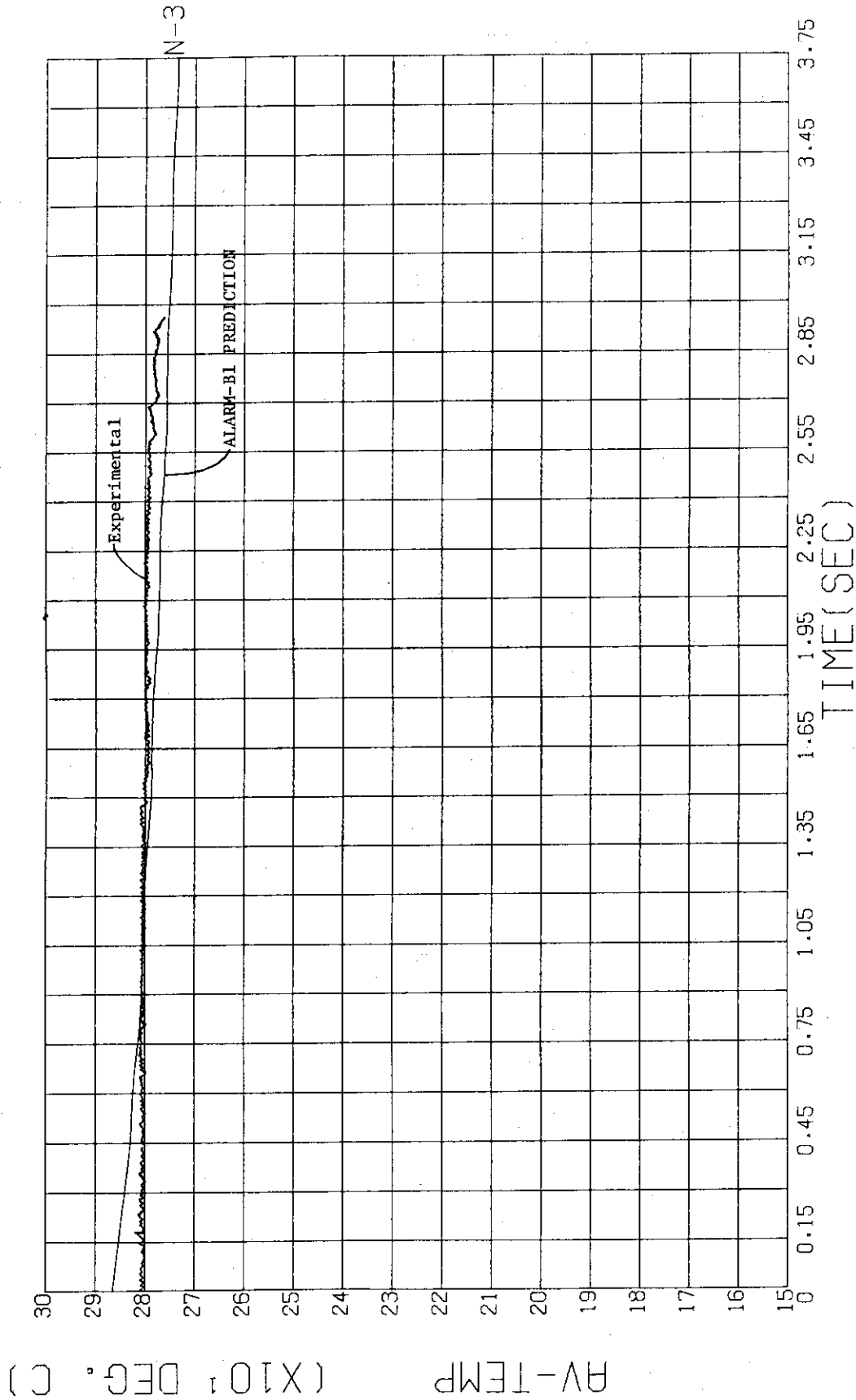


Fig.18 Temperature in the Vessel at Level F (Re-analysis)

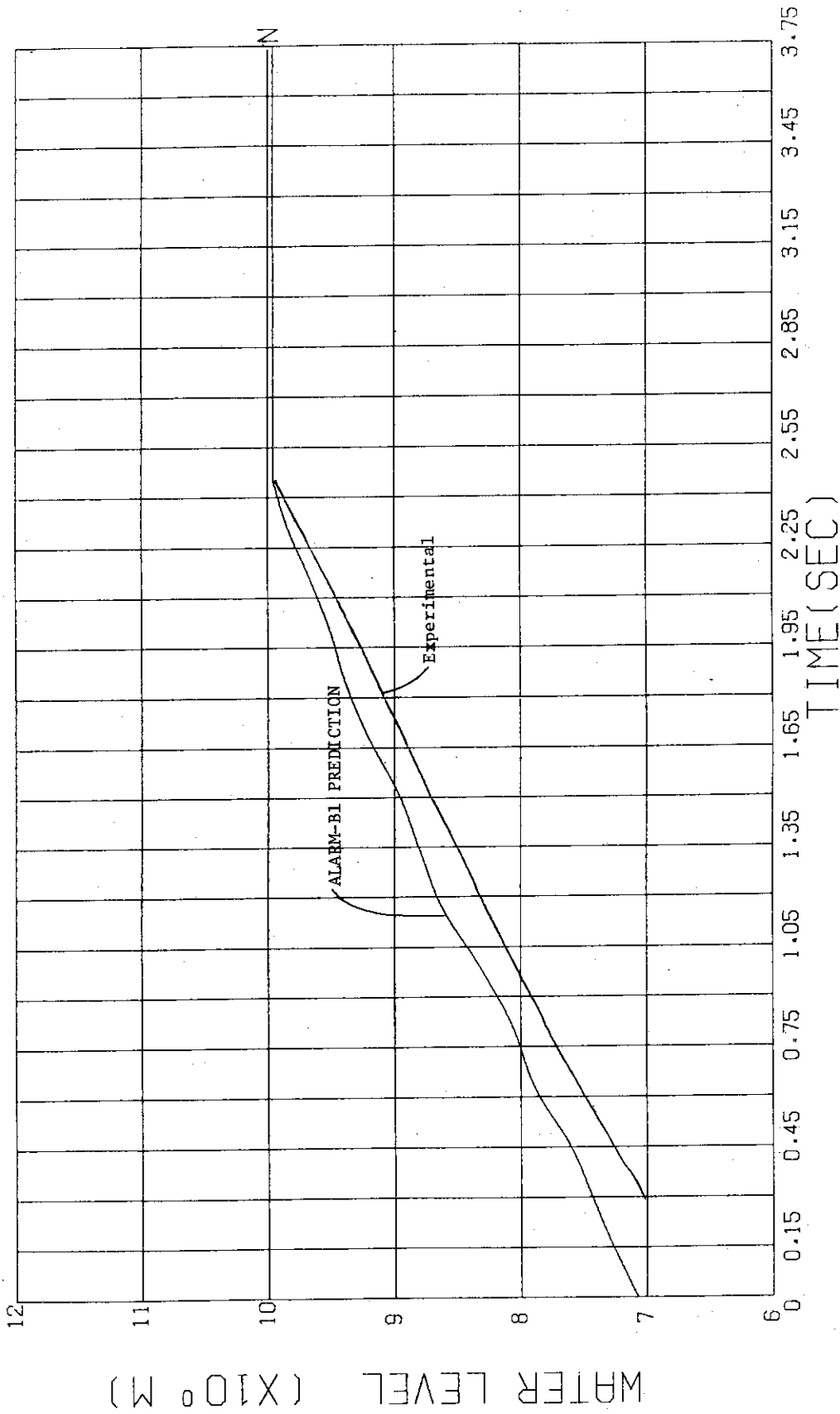


Fig.19 Liquid Level in the Vessel (Re-analysis)

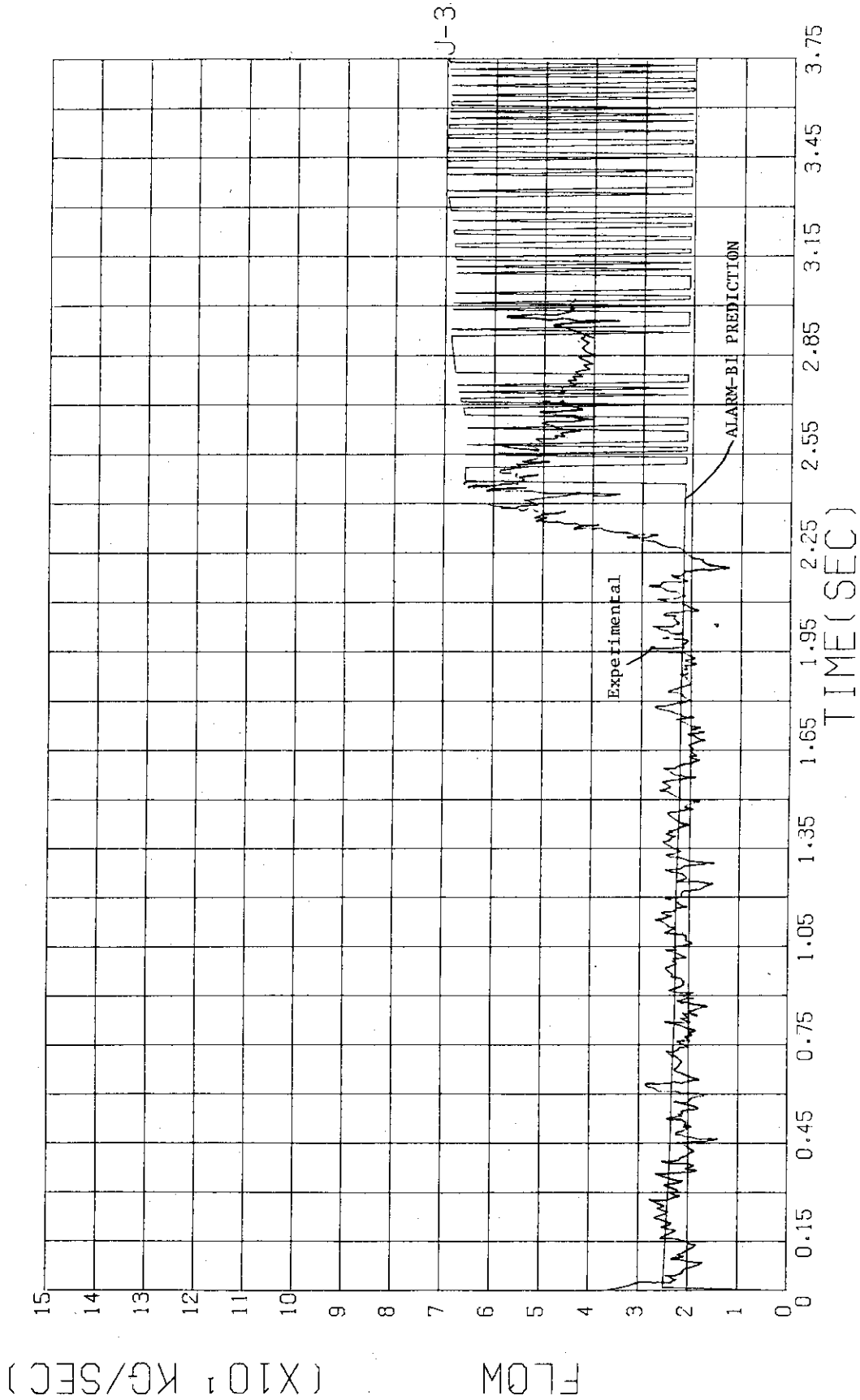


Fig.20 Discharge Mass Flow Rate (Re-analysis)

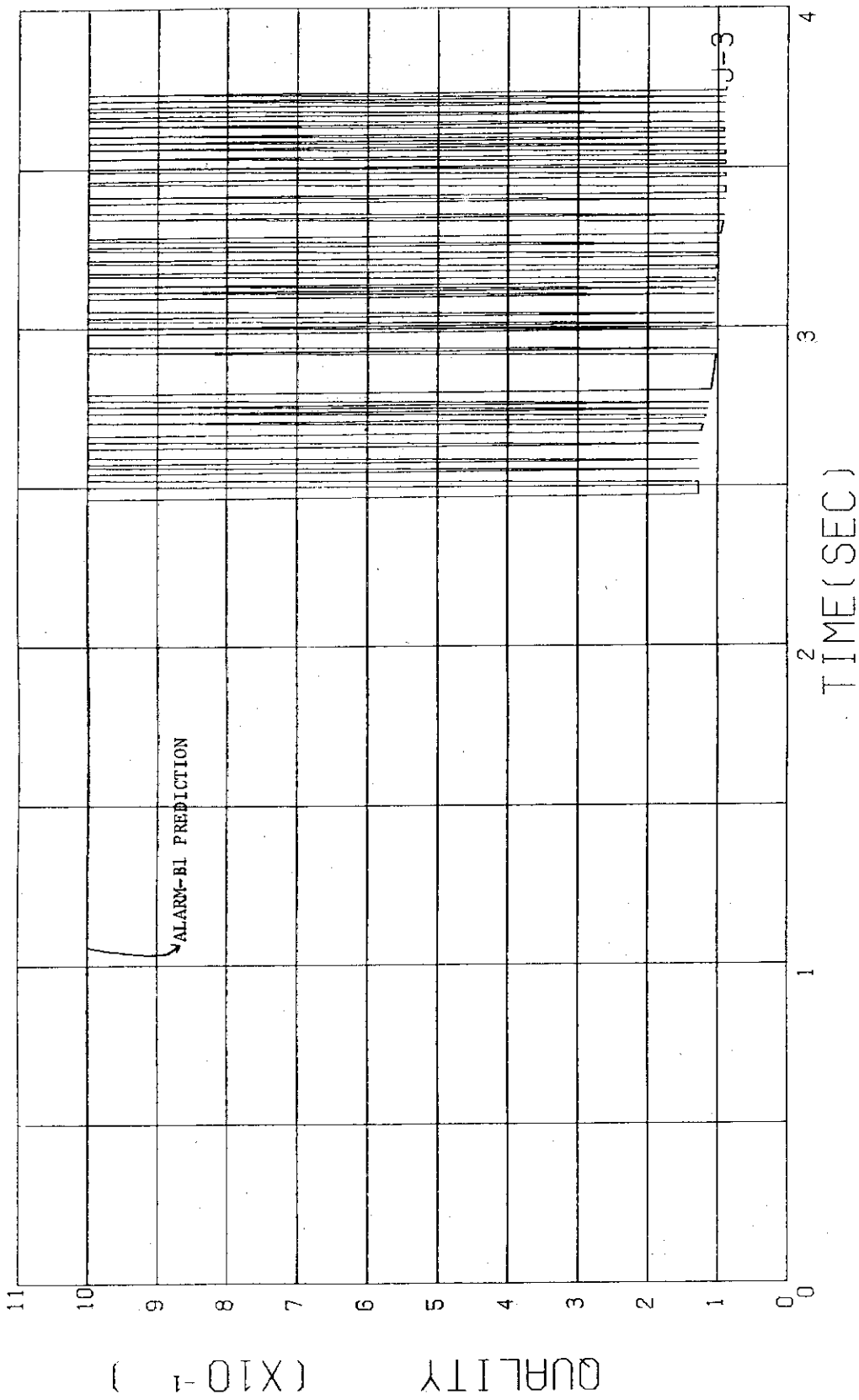


Fig.21 Flow Quality at Outlet (Re-analysis)

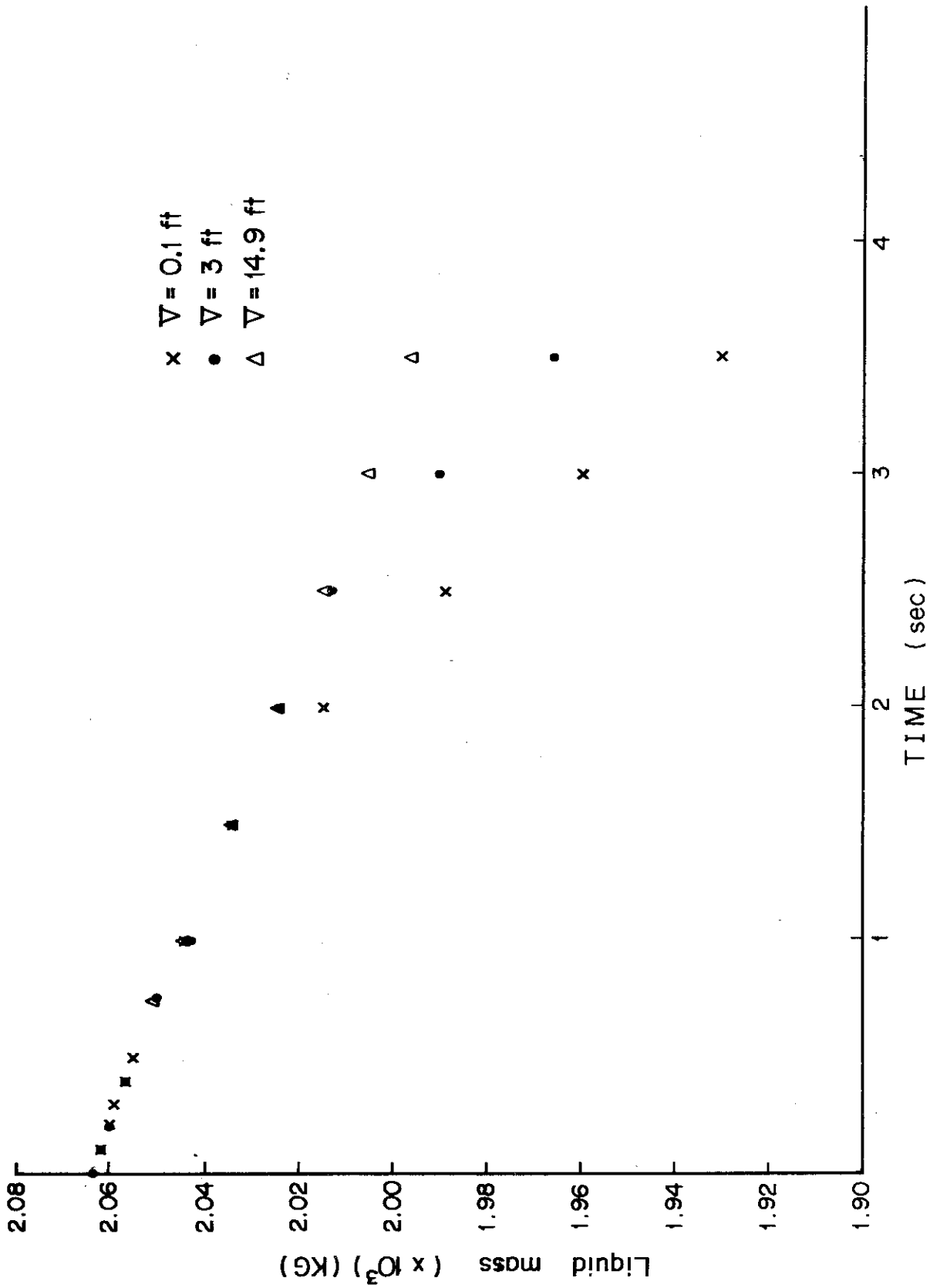


Fig.22 Mass Inventory in the Vessel (Re-analysis)

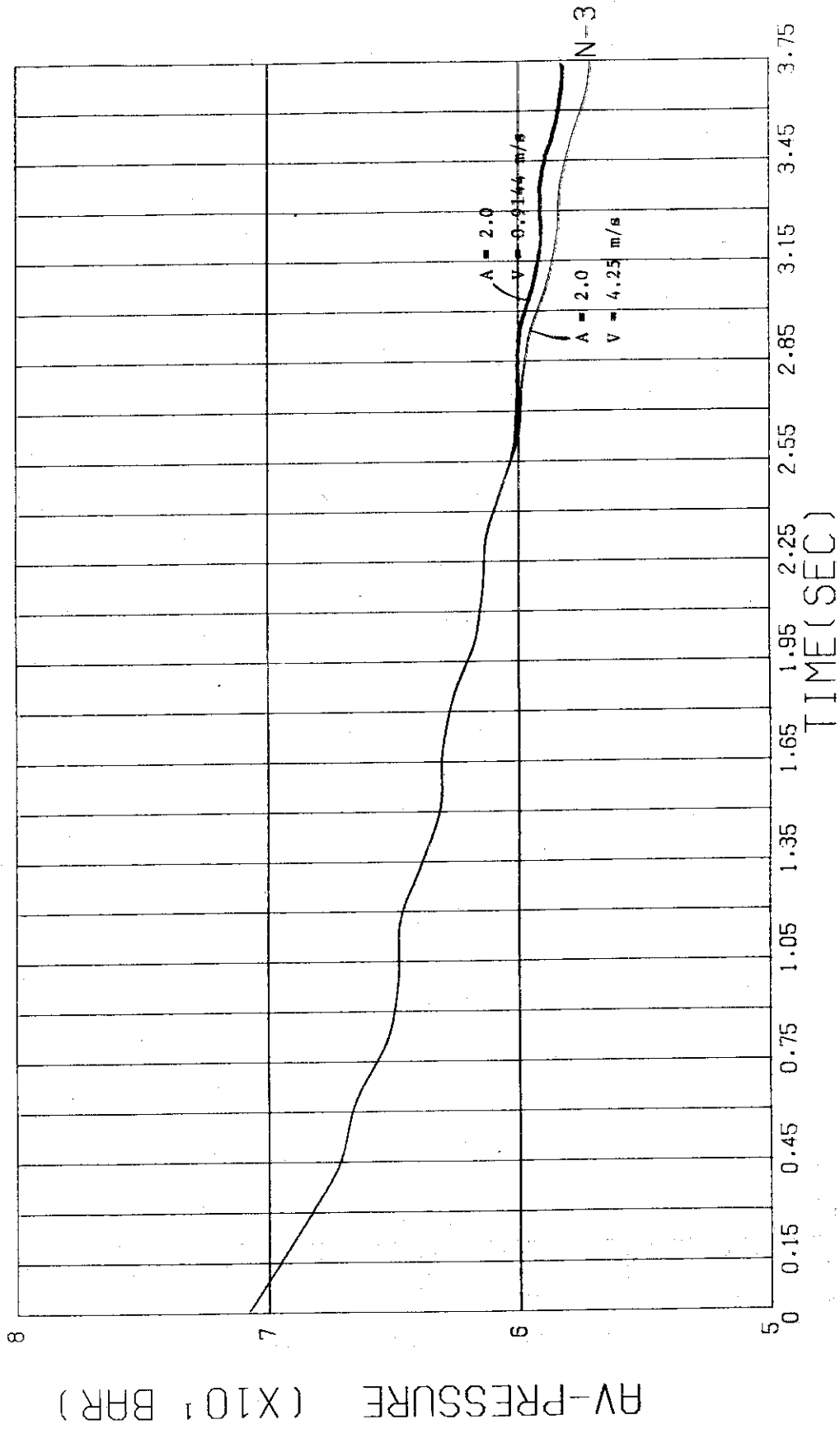


Fig.23 Pressure Profiles due to Bubble Parameters (Re-analysis)

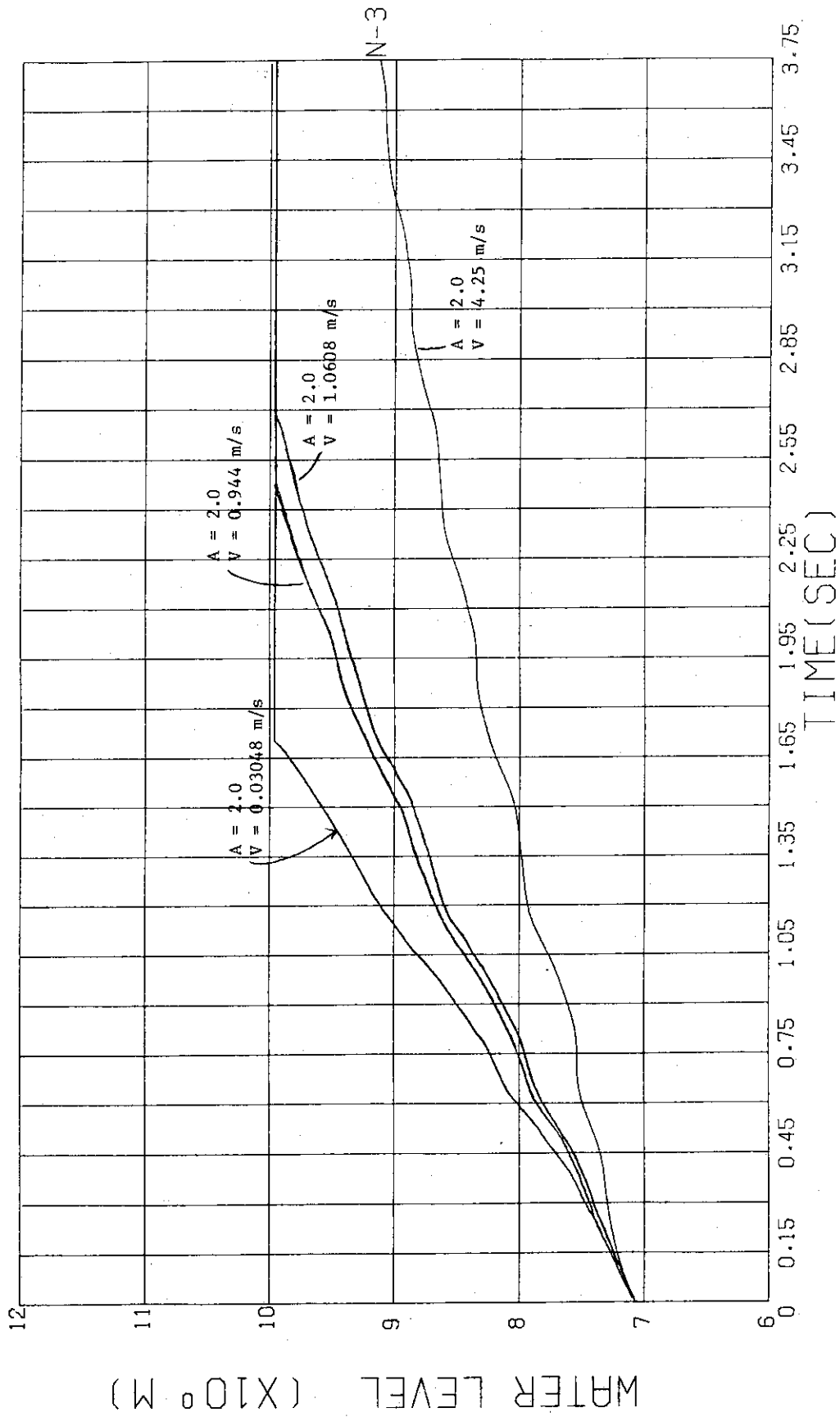


Fig.24 Water Level Profiles due to Bubble Parameters
(Re-analysis)

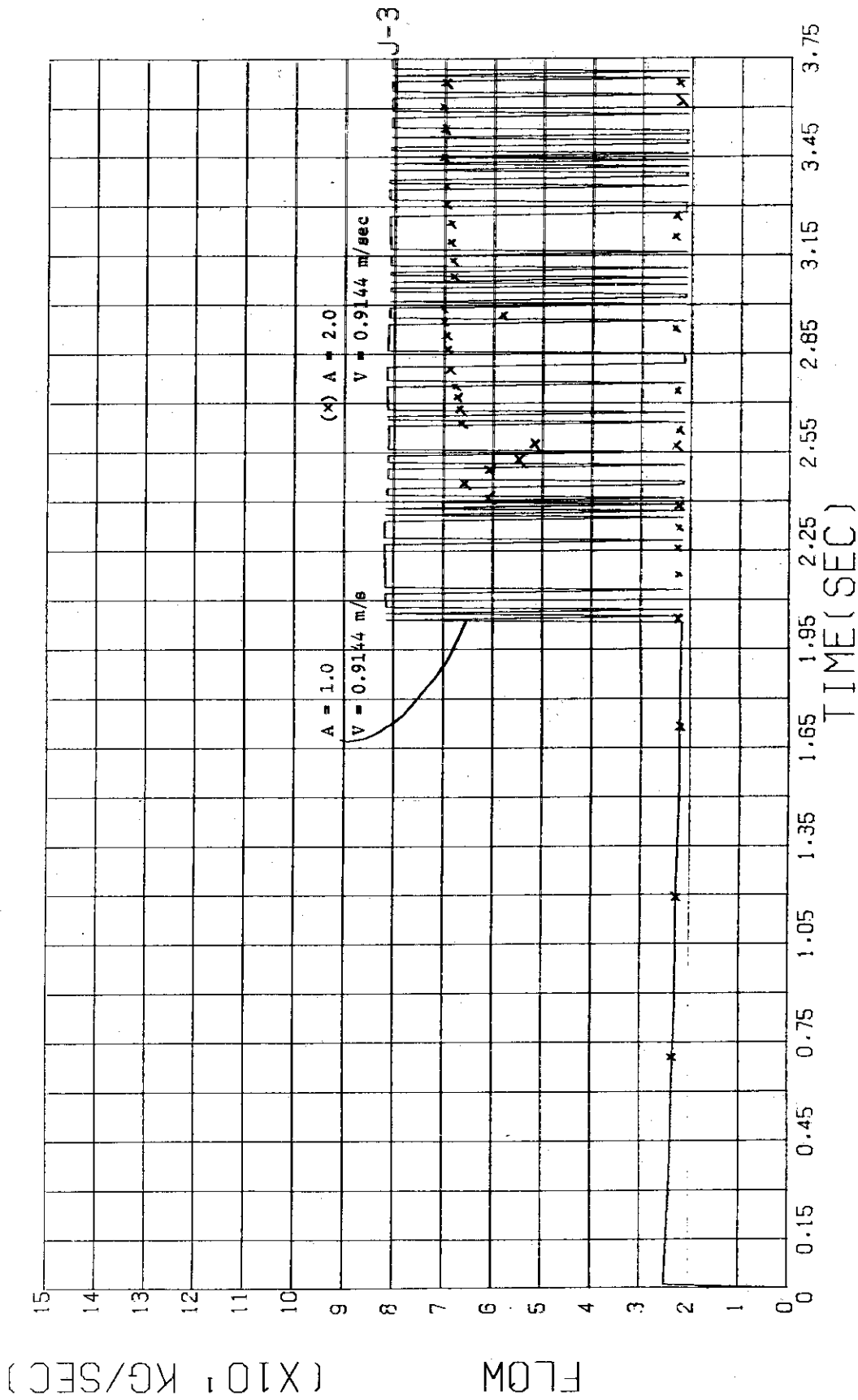


Fig.25 Discharge Flow Profiles due to Bubble Parameters

(Re-analysis)

STANDARD PROBLEM NO.6

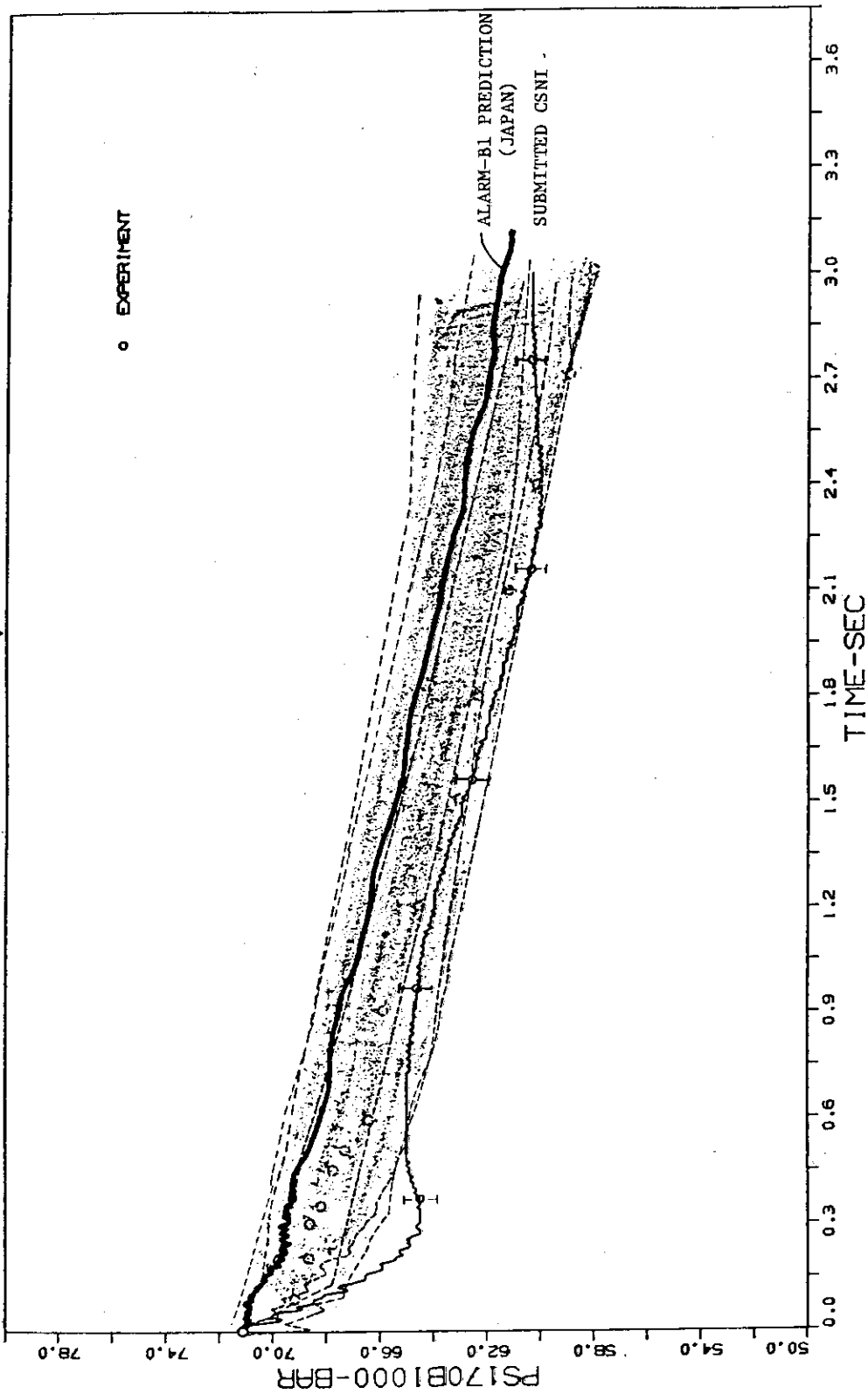


Fig.26 Envelope of Pressure Predictions at Level B

STANDARD PROBLEM NO.6

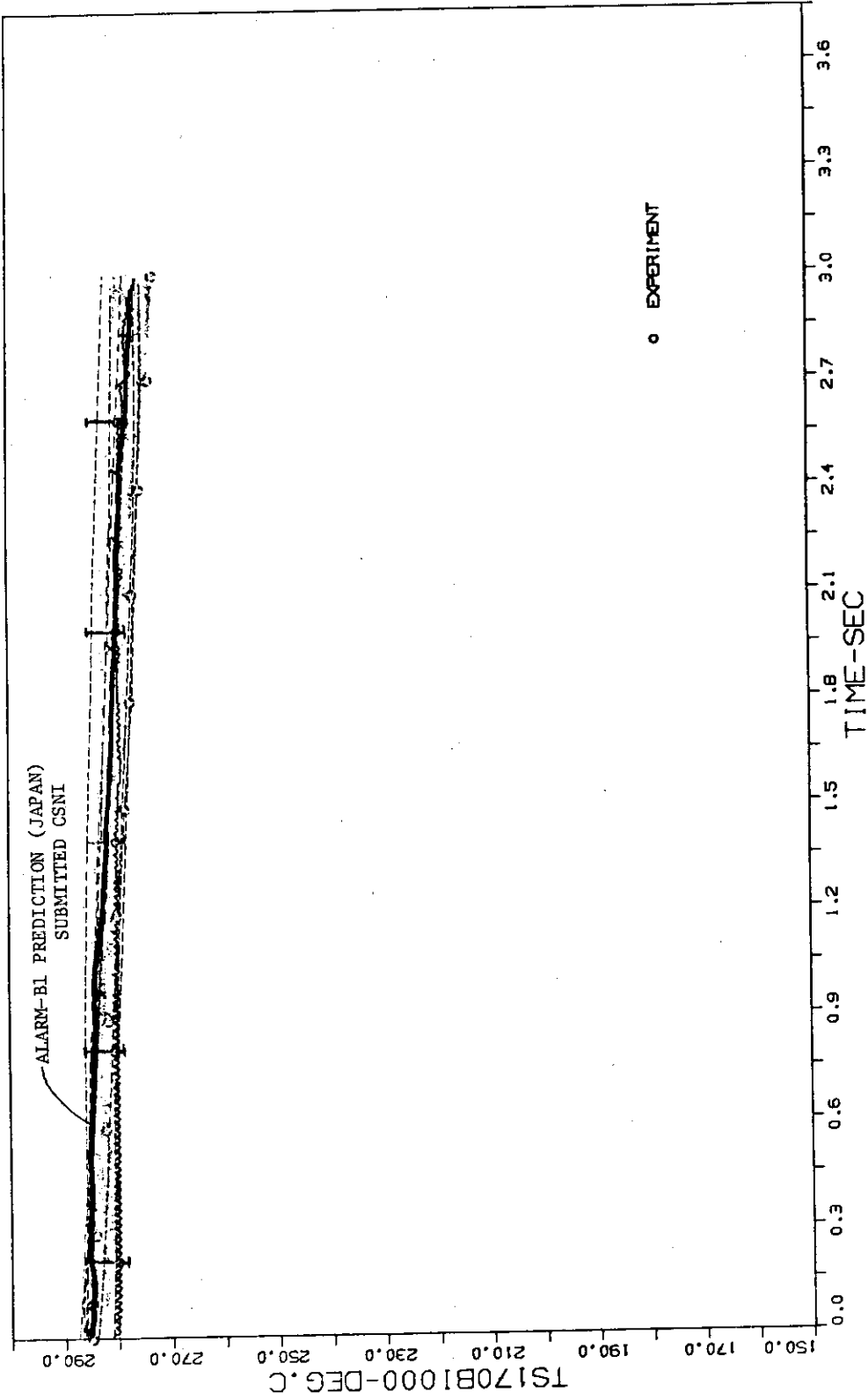


Fig.27 Envelope of Temperature Predictions at Level B

STANDARD PROBLEM NO.6

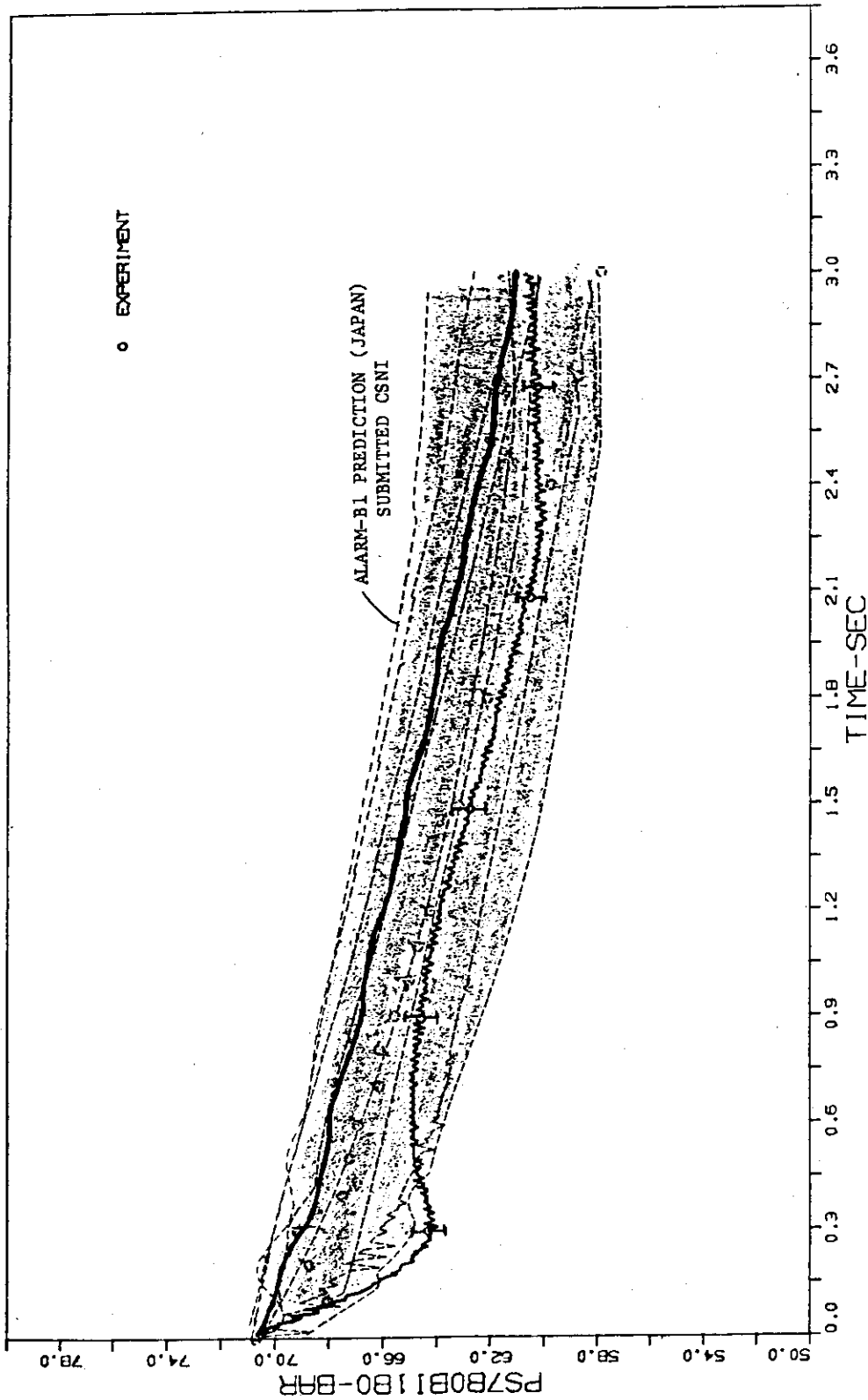


Fig.28 Envelope of Pressure Predictions at Level F

STANDARD PROBLEM NO.6

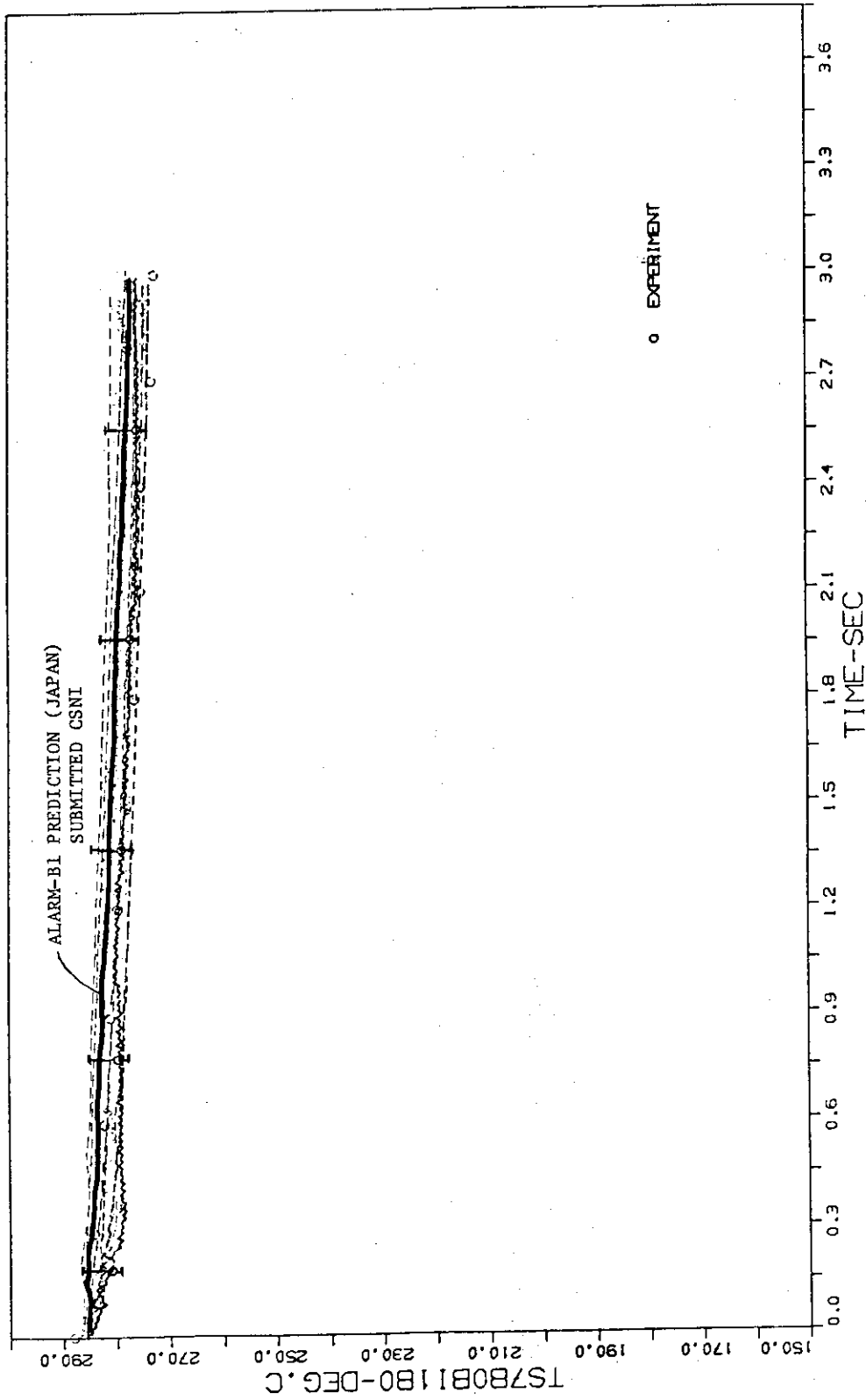


Fig.29 Envelope Temperature Predictions at Level F

STANDARD PROBLEM NO.6

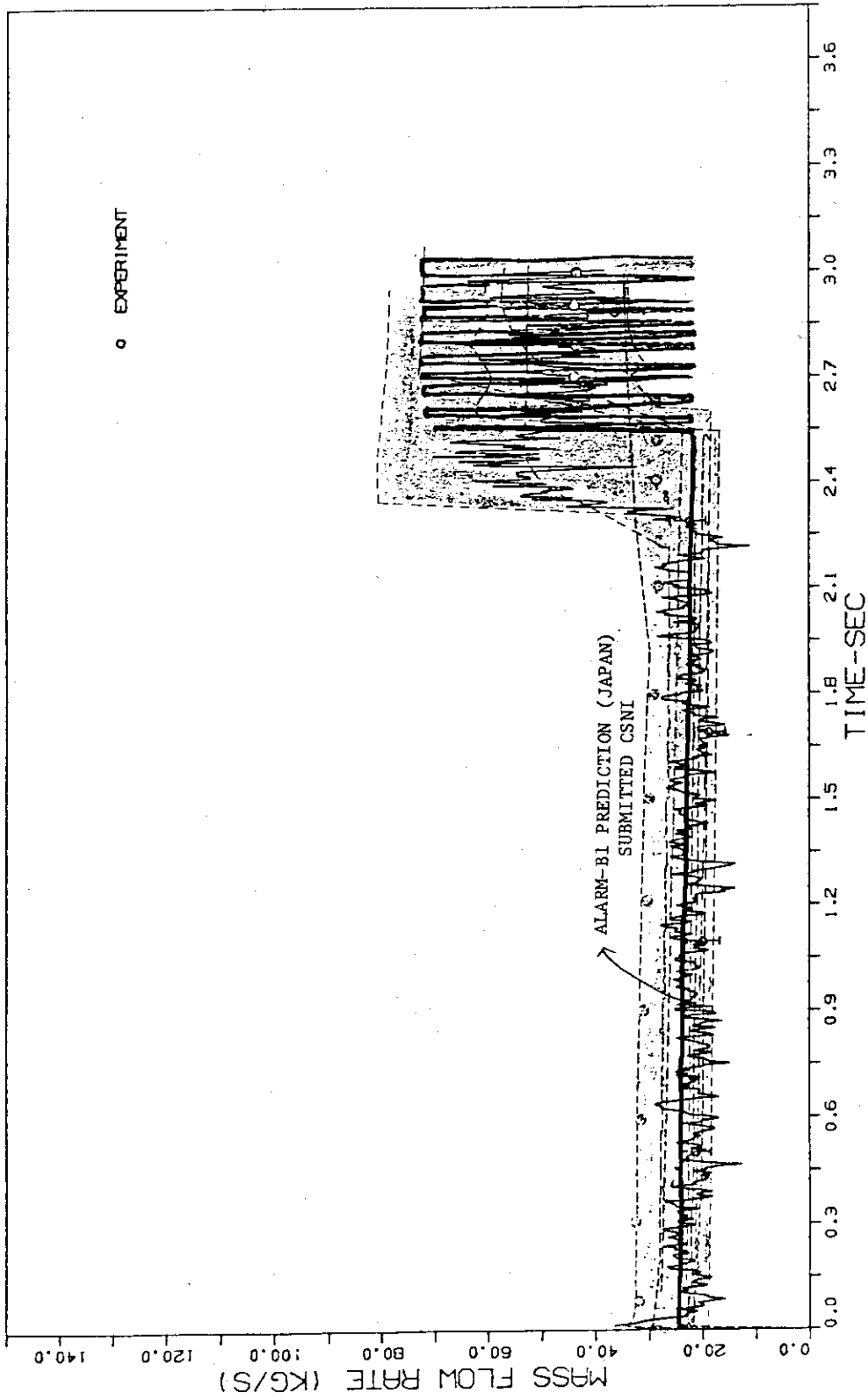


Fig.30 Envelope of Mass Flow Rate Predictions in the Discharge
Nozzle

STANDARD PROBLEM NO.6

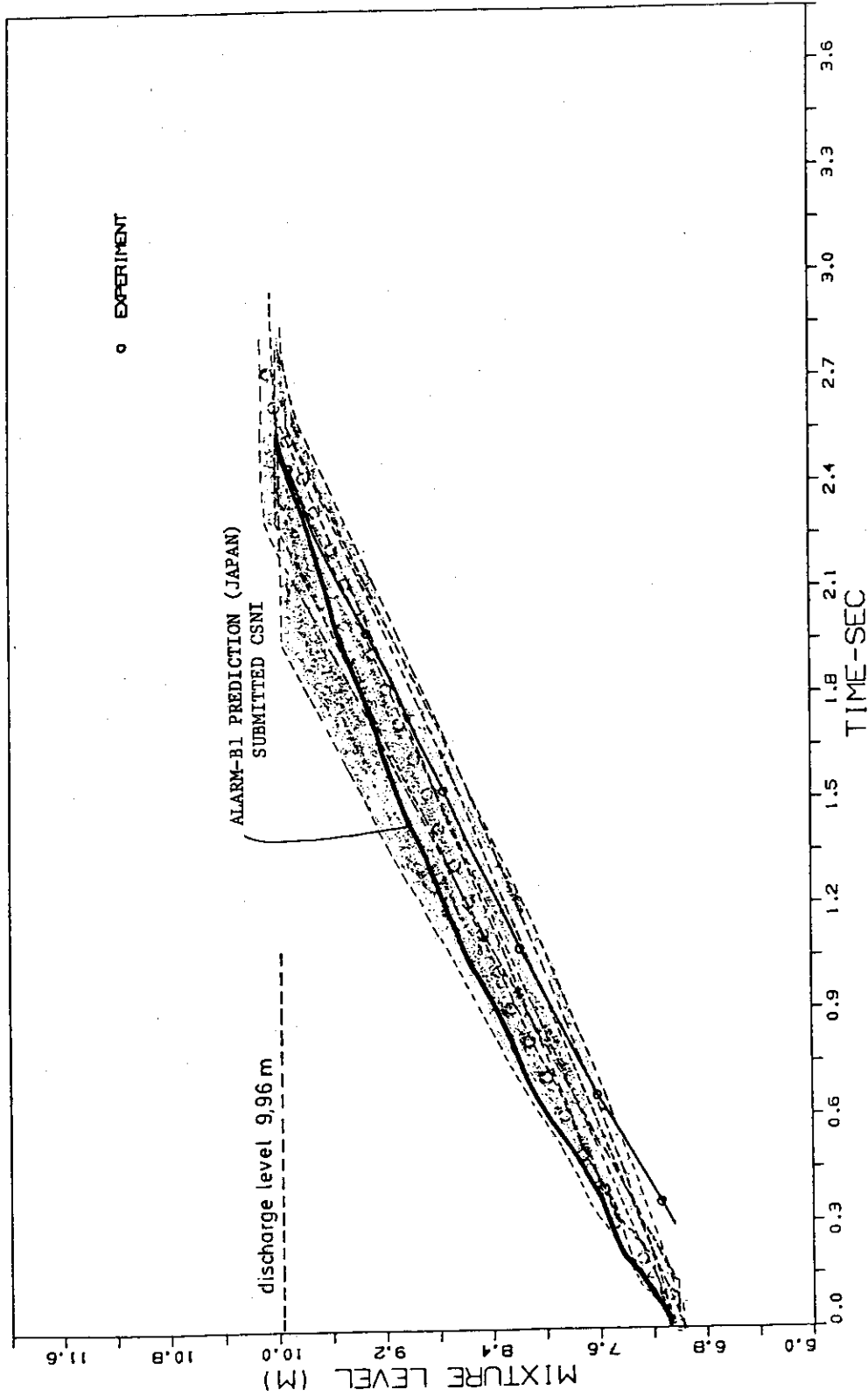


Fig.31 Envelope of Mixture Level Predictions

Appendices

- (1) ALARM-B1 input data
- (2) ALARM-B1 input data (Re-analysis)
- (3) Calculated results of participants
- (4) ALARM-B1 plotter routine

Appendix 1. ALARM-B1 input data

```

***** LISTING OF INPUT DATA *****
NO. ....*.....1.....*.....2.....*.....3.....*.....4.....*.....5.....*.....6.....*.....7.....*.....8
1      CSNI STANDARD PROBLEM NO.6 ANALYSIS BY ALARM-B1                                ISP60000
2      /* PRESSURE GAUGES                                                            ISP60010
3      /* PS170B1000 = PRESSURE OF NODE1                                           ISP60020
4      /* PS380B1000 = PRESSURE OF NODE2                                           ISP60030
5      /* PS780B1180 = PRESSURE OF NODE3                                           ISP60040
6      /*                                                                            ISP60050
7      /* TEMPERATURE GAUGES                                                       ISP60060
8      /* TS170B1000 = TEMPERATURE OF NODE1                                        ISP60070
9      /* TS380B1000 = TEMPERATURE OF NODE2                                        ISP60080
10     /* TS780B1180 = TEMPERATURE OF NODE3                                        ISP60090
11     1 / PROBLEM DIMENSION                                                         ISP60100
12     0 8 3 2 3 1 3 0 1 5(0) 8 160                                               ISP60110
13     /*                                                                            ISP60120
14     2 / EDIT VARIABLE                                                             ISP60130
15     /*                                                                            ISP60140
16     AP N1 AP N2 AP N3 AT N1 AT N2 AT N3 ZM N3 JF J3                             ISP60150
17     /*                                                                            ISP60160
18     3 / TIME STEP                                                                ISP60170
19     /*                                                                            ISP60180
20     100 5 0 100 0.0001 0.5                                                       ISP60190
21     50 10 0 20 0.0005 1.0                                                       ISP60200
22     10 50 0 10 0.001 3.75                                                       ISP60210
23     /*                                                                            ISP60220
24     4 / TRIP CONTROL                                                             ISP60230
25     /*                                                                            ISP60240
26     1 1 0 0 4.00 0.0                                                            ISP60250
27     2 1 0 0 0.0001 0.0                                                           ISP60260
28     /*                                                                            ISP60270
29     5 / VOLUME                                                                    ISP60280
30     /*                                                                            ISP60300
31     0 0 0 0 0 72.369E4 285.0 1.2433 2.67 2.67 2(0.0) ISP60310
32     0 0 0 0 0 72.232E4 0.0 0.5998 2.33 2.33 ISP60320
33     2.67 0.0 ISP60330
34     1 0 0 0 0 72.205E4 0.0 2.8801 6.185 2.07 ISP60340
35     5.00 0.0 ISP60350
36     /*                                                                            ISP60360
37     6 / BUBBLE DATA                                                             ISP60370
38     /*                                                                            ISP60380
39     2.0 1.21920                                                                    ISP60390
40     /*                                                                            ISP60400
41     7 / JUNCTION DATA                                                           ISP60410
42     /*                                                                            ISP60420
43     1 2 0 0 0.0 0.2574 0.078 0.2574 2.67 2.67 7.39 2(0.0) ISP60430
44     2 3 0 0 0.0 0.2574 0.078 0.2574 2.33 5.00 10.32 2(0.0) ISP60440
45     3 -1 1 0 0.0 3.217E-3 0.064 3.217E-3 5.40 9.983 5.80 2(0.0) ISP60450
46     /*                                                                            ISP60460
47     11 / LEAK DATA                                                             ISP60470
48     /*                                                                            ISP60480
49     3 0 1.0E4 0.75                                                                ISP60490
50     0.0 0.0 0.0001 1.0 5.0 1.0                                                 ISP60500
51     /*                                                                            ISP60510
52     15 / PLCT DATA                                                             ISP60520
53     /*                                                                            ISP60530
54     250.0 150.0                                                                    ISP60540
55     AP N1 AP N2 AP N3 AT N1 AT N2 AT N3 ZM N3 JF J3                             ISP60550
56     0                                                                            ISP60560
57     END                                                                            ISP60570

```

END OF INPUT DATA

Appendix 2. ALARM-B1 input data (Re-analysis)

```

***** LISTING OF INPUT DATA *****
NO. ....*.....1.....*.....2.....*.....3.....*.....4.....*.....5.....*.....6.....*.....7.....*.....8
1          CSNI STANDARD PROBLEM NO.6 ANALYSIS BY ALARM-B1                                ISP60000
2          /* PRESSURE GAUGES                                                            ISP60010
3          /* PS170B1000 = PRESSURE OF NODE1                                           ISP60020
4          /* PS380B1000 = PRESSURE OF NODE2                                           ISP60030
5          /* PS780B1180 = PRESSURE OF NODE3                                           ISP60040
6          /*                                                                            ISP60050
7          /* TEMPERATURE GAUGES                                                         ISP60060
8          /* TS170B1000 = TEMPERATURE OF NODE1                                       ISP60070
9          /* TS380B1000 = TEMPERATURE OF NODE2                                       ISP60080
10         /* TS780B1180 = TEMPERATURE OF NODE3                                       ISP60090
11         1 / PROBLEM DIMENSION                                                         ISP60100
12         0  8  3  2  3  1  3  0  1  5(0)  8  160                                     ISP60110
13         /*                                                                            ISP60120
14         2 / EDIT VARIABLE                                                             ISP60130
15         /*                                                                            ISP60140
16         AP N1 AP N2 AP N3 AT N1 AT N2 AT N3 ZM N3 JF J3                             ISP60150
17         /*                                                                            ISP60160
18         3 / TIME STEP                                                                 ISP60170
19         /*                                                                            ISP60180
20         /*                                                                            ISP60190
21         100      5      0      100      0.0001      0.5                             ISP60200
22         50      10     0      20      0.0005      1.0                             ISP60210
23         10      50     0      10      0.001       3.75                             ISP60220
24         /*                                                                            ISP60230
25         4 / TRIP CONTROL                                                             ISP60240
26         /*                                                                            ISP60250
27         1      1      0      0      4.00      0.0                             ISP60260
28         2      1      0      0      0.0001     0.0                             ISP60270
29         /*                                                                            ISP60280
30         5 / VOLUME                                                                    ISP60290
31         /*                                                                            ISP60300
32         0  0  0  0  0  72.369E4  282.0  1.2526  2.69  2.69  2(0.0) ISP60310
33         0  0  0  0  0  72.232E4  284.0  0.6436  2.50  2.50                             ISP60320
34         2.69  0.0                                     ISP60330
35         1  0  0  0  0  72.205E4  0.0  2.8016  6.000  1.88                       ISP60340
36         5.19  0.0                                     ISP60350
37         /*                                                                            ISP60360
38         6 / BUBBLE DATA                                                             ISP60370
39         /*                                                                            ISP60380
40         1.0      0.9144                                                             ISP60390
41         /*                                                                            ISP60400
42         7 / JUNCTION DATA                                                           ISP60410
43         /*                                                                            ISP60420
44         1  2  0  0  0.0  0.2574  0.082  0.2574  2.69  2.69  12.43  2(0.0) ISP60430
45         2  3  0  0  0.0  0.2574  0.082  0.2574  2.50  5.19  17.97  2(0.0) ISP60440
46         3 -1  1  0  0.0  3.217E-3  0.064  3.217E-3  5.27  9.96  44.45  2(0.0) ISP60450
47         /*                                                                            ISP60460
48         11 / LEAK DATA                                                             ISP60470
49         /*                                                                            ISP60480
50         3      0      1.0E4      0.75                                             ISP60490
51         0.0      0.0      0.0001      1.0  5.0      1.0                             ISP60500
52         /*                                                                            ISP60510
53         15 / PLOT DATA                                                             ISP60520
54         /*                                                                            ISP60530
55         250.0      150.0                                                           ISP60540
56         AP N1 AP N2 AP N3 AT N1 AT N2 AT N3 ZM N3 JF J3                             ISP60550
57         0                                                                            ISP60560
58         END                                                                           ISP60570

```

END OF INPUT DATA

Table 4 Calculated Results of Participants

Country	Code	Calculated results for											discharge mass flow rate				
		pressure at level					temperature at level					charge nozzle		temperature in discharge nozzle	mixture level		
		B	C	E	F	G	B	C	E	F	G	pressure in discharge nozzle	temperature in discharge nozzle	discharge nozzle	mixture level	discharge mass flow rate	
Finland Germany UK (UKAEA)	a) non-equilibrium																
	NORA	X	X	X	X	O	X	X	X	X	O	O	X	O	X	X	X
	DFUFAN FROTH2	X	X	X	X	O	X	X	X	X	O	X	X	X	X	X	X
Australia Germany Italy (CNEN) Italy (Nuclital) Japan Sweden Switzerland UK (UKAEA) UK (Strathclyde) US France*	b) equilibrium																
	NAIAD	X	X	X	X	X	X	X	X	X	X	X	X	X	X	X	
	BRUCH-S RELAP-UK RELAP4/MOD5 RELAP4/MOD5*	X X O O	X X X X	O X O X	O X O X	O X O X	X X X X	X X X X	X X X X	X X X X	X X X X	X X X X	X X X X	X X X X	X X X X	X X X X	X X X X
	ALARM-B1 RELAP4/MOD3(95) RELAP4/MOD2 RELAP-UK Mk III RELAP4/MOD3(WREM) RELAP4/MOD5(2) RELAP4/MOD5	X X X X X X X	X X X X X X X	O X O X O X X	O X O X O X X	O X O X O X X	X X X X X X X	X X X X X X X	X X X X X X X	X X X X X X X	X X X X X X X	X X X X X X X	X X X X X X X	X X X X X X X	X X X X X X X	X X X X X X X	X X X X X X X

X = calculated
O = not calculated
↑ = taken for comparison

* calculations submitted after deadline to the workshop on CSNI LOCA Standard Problems at Garching, April 11-14, 1978
** post calculation

Appendix 4. ALARM-B1 plotter routine

FACOM 230-75 (M7)

LIBE 77.11.21 (V-03 L-12)

79/05/29

PAGE-0002

SOURCE ELEMENT LIST (SRIT MODE)

ELEMENT NAME ((PLOTER)) ESTABLISHED 78.09.28

```

SUBROUTINE PLOTER ( XPL0T,XMIN,XMAX,LSEQ,NSEQ,NBF,NEDP,NEDP1, PLO00010
* LSEQ,NSEQ,NUM,YLAST,TLAST) PLO00020
REAL*8 YLAST,TLAST,TIME,DAT PLO00030
COMMON / PDIM / PLO00040
1 NRPST , NEDIT , NTSC , NTRIP , NVOL , NBUB , NJUN , PLO00050
2 NPUMP , NL* , NFILL , NSUB , NJETP , NTSUR , NJEGRP , PLO00060
* NEDITP , NBUF , NEDTPI PLO00070
COMMON /TCNT/ KSTEP , NTRAN , TIME PLO00080
COMMON / FORM / PLO00090
* EDUMV( 3,15) , EDUMJ( 3, 7) , EDUMS( 3, 3) , EDUMT( 3, 5) PLO00100
COMMON /COMPL/ KPLT,LPLT,XLEN,YLEN PLO00110
COMMON /TAPF/ ITAPER,ITAPER,ITAPER PLO00120
COMMON TITLE(18),DUMY(40),DAT PLO00130
DIMENSION NUM(1),YLAST(1),TLAST(1),IAUX(100) PLO00140
DIMENSION XPL0T( NBF,NEDP1) , XMIN(NEDP),XMAX(NEDP) , PLO00150
* LSEQ(NEDP) , NSEQ(NEDP) , LSEQN( 1) , NSEQN( 1) PLO00160
COMMON / UNIT / PWR,UNITV(2,15),UNITJ(2, 4),UNITT(3, 2) PLO00170
C PLO00260
C PLO00270
C PLO00280
C PLO00290
C PLO00300
C PLO00310
C PLO00320
C PLO00330
C PLO00340
C PLO00350
C PLO00360
C PLO00370
C PLO00380
C PLO00390
C PLO00400
C PLO00410
C PLO00420
C PLO00430
C PLO00440
C PLO00450
C PLO00460
C PLO00470
C PLO00480
C PLO00490
C PLO00500
C PLO00510
C PLO00520
C PLO00530
C PLO00540
C PLO00550
C PLO00560
C PLO00570
C PLO00580
C PLO00590
C PLO00600
SUBROUTINE PLOTER ( XPL0T,XMIN,XMAX,LSEQ,NSEQ,NBF,NEDP,NEDP1,
* LSEQ,NSEQ,NUM,YLAST,TLAST)
REAL*8 YLAST,TLAST,TIME,DAT
COMMON / PDIM /
1 NRPST , NEDIT , NTSC , NTRIP , NVOL , NBUB , NJUN ,
2 NPUMP , NL* , NFILL , NSUB , NJETP , NTSUR , NJEGRP ,
* NEDITP , NBUF , NEDTPI
COMMON /TCNT/ KSTEP , NTRAN , TIME
COMMON / FORM /
* EDUMV( 3,15) , EDUMJ( 3, 7) , EDUMS( 3, 3) , EDUMT( 3, 5)
COMMON /COMPL/ KPLT,LPLT,XLEN,YLEN
COMMON /TAPF/ ITAPER,ITAPER,ITAPER
COMMON TITLE(18),DUMY(40),DAT
DIMENSION NUM(1),YLAST(1),TLAST(1),IAUX(100)
DIMENSION XPL0T( NBF,NEDP1) , XMIN(NEDP),XMAX(NEDP) ,
* LSEQ(NEDP) , NSEQ(NEDP) , LSEQN( 1) , NSEQN( 1)
COMMON / UNIT / PWR,UNITV(2,15),UNITJ(2, 4),UNITT(3, 2)

PLOTTING ROUTINE
DIMENSION IBUF(1)
REWIND ITAPER

CALL PLOTS(IBUF,IALARM)

IS* = 0
IF ( NREST.LT.0 .AND. NEDITP.EQ.0 ) NEDITP=NEDP

IX = 0
DO 1 I=1,NEDITP
DO 2 J=1,NEDP
IF ( LSEQN(I).EQ.LSEQN(J) .AND. NSEQN(I).EQ.NSEQN(J) ) GO TO 3
2 CONTINUE
GO TO 1
3 CONTINUE
IX = IX + 1
IAUX(IX) = J
1 CONTINUE

IF ( IX.EQ.0 ) GO TO 999

IAX = 0
I = 1
J = 1

XX = XMAX( IAUX(I) )
XN = XMIN( IAUX(I) )
LO = LSEQ( IAUX(I) )

```

Appendix 4. (continued)

FACOM 230-75 (M7)

L I B E 77.11.21 (V-03 L-12)

79/05/29

PAGE-0003

SOURCE ELEMENT LIST (8BIT MODE)

NO = NSEQ(IAX(1))	PLO00610
100 I = I + 1	PLO00620
C	PLO00630
IF (I.GT.IX) GO TO 200	PLO00640
K = IAX(I)	PLO00650
C	PLO00660
200 CONTINUE	PLO00670
IAX = IAX + 1	PLO00680
NUM(IAX) = J	PLO00690
XMIN(IAX) = XN	PLO00700
XMAX(IAX) = XX	PLO00710
IF (I.GT.IX) GO TO 300	PLO00720
J = 1	PLO00730
LU = LSEQ(K)	PLO00740
NO = NSEQ(K)	PLO00750
XN = XMIN(K)	PLO00760
XX = XMAX(K)	PLO00770
GO TO 100	PLO00780
300 CONTINUE	PLO00790
C	PLO00800
DT = 10.0	PLO00810
IF (TIME.LT.100.0) DT=5.0	PLO00820
IF (TIME.LT.10.0) DT=0.5	PLO00830
IF (TIME.LT.1.0) DT=0.05	PLO00840
NDX = TIME/DT + 1	PLO00850
IF (MOD(NDX,2).NE.0) NDX=NDX+1	PLO00860
C	PLO00870
DX = XLEN / (NDX*DT)	PLO00880
DT=0.15	PLO00881
NDX=25	PLO00882
DX=10./0.15	PLO00883
C	PLO00890
C	PLO00900
C PLOTTING	PLO00910
C	PLO00920
K = 0	PLO00930
C	PLO00940
CALL PLOT(0.,0.,3)	PLO00945
DO 400 I=1,IAX	PLO00950
C	PLO00960
C	PLO00970
C SET DX,DY ACCORDING TO XMIN(I),XMAX(I)	PLO00980
C	PLO00990
LPLT1=LPLT	PLO01000
K=K+1	PLO01002
L=IAUX(K)	PLO01004
LL=LSEQ(L)	PLO01006
IF (NSEQ(L).GT.0.AND.LL.E0.1) GO TO 111	PLO01010
IF (NSEQ(L).GT.0.AND.LL.E0.3) GO TO 121	PLO01012
IF (NSEQ(L).GT.0.AND.LL.E0.8) GO TO 131	PLO01014
IF (NSEQ(L).LT.0.AND.LL.E0.1) GO TO 141	PLO01016
STOP 9999	PLO01030
111 CONTINUE	PLO01035
XMIN(I)=50.0	PLO01040

Appendix 4. (continued)

FACOM 230-75 (M7)

L I B E 77.11.21 (V-03 L-12)

79/05/29

PAGE-0004

SOURCE ELEMENT LIST (8BIT MODE)

	NDY2=8	PLO01045
	NDY1=5	PLO01050
	XS=10.0	PLO01055
	NX=NDY2-NDY1	PLO01060
	XMAX(I)=YLEN/(NX*XS)	PLO01065
	GO TO 11111	PLO01070
121	CONTINUE	PLO01075
	XMIN(I)=150.0	PLO01080
	NDY2=30	PLO01085
	NDY1=15	PLO01090
	XS=10.0	PLO01095
	NX=NDY2-NDY1	PLO01100
	XMAX(I)=YLEN/(NX*XS)	PLO01105
	GO TO 11111	PLO01110
131	CONTINUE	PLO01115
	XMIN(I)=6.0	PLO01120
	NDY2=12	PLO01125
	NDY1=6	PLO01130
	XS=1.0	PLO01135
	NX=NDY2-NDY1	PLO01140
	XMAX(I)=YLEN/(NX*XS)	PLO01145
	GO TO 11111	PLO01150
141	CONTINUE	PLO01152
	XMIN(I)=0.0	PLO01154
	NDY2=15	PLO01156
	NDY1=0	PLO01157
	XS=10.0	PLO01159
	NX=NDY2-NDY1	PLO01160
	XMAX(I)=YLEN/(XS*NX)	PLO01162
11111	CONTINUE	PLO01163
C		PLO01170
	X = XLEN	PLO01180
	CALL PLOT (X,0.,.2)	PLO01190
	DO 480 N=1,NDX	PLO01200
	CALL PLOT(X,YLEN*.3)	PLO01210
	CALL PLOT(X,0.,.2)	PLO01220
	IF (MOD(N,2).EQ.0) GO TO 481	PLO01230
	CALL NUMBER (X-3.,-5.,.3., (NDX-N+1)*DT ,0.,.2)	PLO01240
481	CONTINUE	PLO01250
	X = X-DT*DX	PLO01260
480	CONTINUE	PLO01270
C		PLO01280
	CALL NUMBER (-3.,-5.,.3.,.0.,.0.,-1)	PLO01290
C		PLO01300
	DY = YLEN / NX	PLO01310
	RNDY1 = FLOAT(NDY1)	PLO01320
	CALL NUMBER (-5.,-1.,.3.,RNDY1,0.,-1)	PLO01330
	DO 485 N=1,NX	PLO01340
	X = DY * FLOAT(N)	PLO01350
	IF (NDY1+N.EQ.0) GO TO 486	PLO01360
	CALL PLOT(XLEN,X*.3)	PLO01370
	GO TO 487	PLO01380
486	CONTINUE	PLO01390
	CALL PLOT (XLEN*X*.3)	PLO01400

Appendix 4. (continued)

FACOM 230-75 (M7)

L I B E 77.11.21 (V-03 L-12)

79/05/29

PAGE-0005

SOURCE ELEMENT LIST (RBIT MODE)

487	CONTINUE	PLO01410
	CALL PLOT(0.,X,2)	PLO01420
	RNDY1 = FLOAT(RNDY1+N)	PLO01430
	CALL NUMBER (-5.,X-1.,3.,RNDY1,0.,-1)	PLO01440
485	CONTINUE	PLO01450
	PW = ALOG10(XS)	PLO01460
C		PLO01470
	CALL PLOT (0.,YLEN,3)	PLO01480
	CALL PLOT (0.,0.,2)	PLO01490
	ISW=0	PLO01500
C		PLO01530
470	CONTINUE	PLO01540
	READ(ITAPEP,END=509) XPLO	PLO01550
	LPLT1=LPLT1-NBF	PLO01560
C		PLO01570
	DY = XMAX(I)	PLO01580
C		PLO01590
	NM = NUM(I)	PLO01600
C		PLO01610
	DC 500 J=1,NM	PLO01620
	L = I AUX(K)	PLO01630
	IF (ISW.NE.0 .OR. J.NE.1) GO TO 505	PLO01640
	LL = LSEQ(L)	PLO01650
	IF (NSEQ(L)) 502,503,501	PLO01660
501	CONTINUE	PLO01670
	CALL SYMBOL (-15.0,YLEN/7.,6.0,EDUMV(1,LL),90.,12)	PLO01680
	GO TO 504	PLO01690
502	CONTINUE	PLO01700
	CALL SYMBOL (-15.0,YLEN/7.0+6.0,EDUMJ(1,LL),90.,12)	PLO01710
	GO TO 504	PLO01720
503	CONTINUE	PLO01730
	CALL SYMBOL (-15.0,YLEN/7.,6.0,EDUMT(1,LL),90.,12)	PLO01740
504	CONTINUE	PLO01750
	CALL SYMBOL (-15.0,YLEN/7.0+72.0+6.0,PWR,90.,4)	PLO01760
	IF (NSEQ(L)) 702,704,701	PLO01770
701	CONTINUE	PLO01780
	IF (LL.EQ.1 .OR. LL.EQ.14) PW=PW	PLO01790
	CALL NUMBER (-18.0,YLEN/7.0+94.0+3.0,PW,90.,-1)	PLO01800
	CALL SYMBOL (-15.0,YLEN/7.0+102.0+6.0,UNITV(1,LL),90.,8)	PLO01810
	GO TO 707	PLO01820
702	CONTINUE	PLO01830
	IF (LL.LT.4) GO TO 703	PLO01840
	PW = PW	PLO01850
	LL = 4	PLO01860
703	CALL NUMBER (-18.0,YLEN/7.0+94.0+3.0,PW,90.,-1)	PLO01870
	CALL SYMBOL (-15.0,YLEN/7.0+102.0+6.0,UNITJ(1,LL),90.,8)	PLO01880
	GO TO 707	PLO01890
704	CONTINUE	PLO01900
	IF (LL.EN.3 .OR. LL.EQ.5) GO TO 705	PLO01910
	LL = 1	PLO01920
	GO TO 706	PLO01930
705	LL = 2	PLO01940
706	CALL NUMBER (-18.0,YLEN/7.0+94.0+3.0,PW,90.,-1)	PLO01950
	CALL SYMBOL (-15.0,YLEN/7.0+102.0+6.0,UNITT(1,LL),90.,9)	PLO01960

Appendix 4. (continued)

FACOM 230-75 (M7)

L I B E 77.11.21 (V-03 L-12)

79/05/29

PAGE=0006

SOURCE ELEMENT LIST (8BIT MODE)

707	CONTINUE	
	CALL SYMBOL (XLEN/2,-10,0,-13,0,6,.'TIME(SEC)',0.,9)	PL001970
505	CONTINUE	PL001980
	IF (ISW.EQ.0) GO TO 510	PL001990
	XLST = TLAST(K)	PL002000
	YLST = YLAST(K)	PL002010
	NS = 1	PL002020
	GO TO 520	PL002030
510	CONTINUE	PL002040
	IF (NSE@(L).GT.0.AND.LL.EQ.1) XPL0T(1,L)=XPL0T(1,L)/1.01972E4	PL002050
	IF (NSE@(L).GT.0.AND.LL.EQ.8) XPL0T(1,L)=XPL0T(1,L)+5.19	PL002052
	XLST = XPL0T (1,NEDP1)	PL002054
	YLST = XPL0T (1,L)	PL002060
	TIME0 = XLST	PL002070
	NS = 2	PL002080
470	CONTINUE	PL002090
	X = DX*XLST	PL002100
	Y = DY*(YLST-XMIN(I))	PL002110
C		PL002120
	CALL FLOT(X,Y,3)	PL002130
C		PL002140
	NB = NBF	PL002150
	IF (LPLT1.LE.0) NB=LPLT1+NBF	PL002160
C		PL002170
	DO 600 N=NS,NB	PL002180
	IF (NSE@(L).GT.0.AND.LL.EQ.1) XPL0T(N,L)=XPL0T(N,L)/1.01972E4	PL002190
	IF (NSE@(L).GT.0.AND.LL.EQ.8) XPL0T(N,L)=XPL0T(N,L)+5.19	PL002192
	XLST = XPL0T (N,NEDP1)	PL002196
	Y = DY*(XPL0T(N,L)-XMIN(I))	PL002200
	CALL PLOT (X,Y,2)	PL002210
600	CONTINUE	PL002220
	TLAST(K) = XPL0T(NB,NEDP1)	PL002230
	YLAST(K) = XPL0T (NB,L)	PL002240
	IF (LPLT1.GT.0) GO TO 508	PL002250
	IF (NSE@(L)) 507,508,506	PL002260
506	CONTINUE	PL002270
	CALL SYMBOL (X+1.,Y-1.,4,.'N-',0.,2)	PL002280
	RNSE@ = FLOAT(NSE@(L))	PL002290
	CALL NUMBER (X+8.,Y-1.,4,RNSE@,0.,-1)	PL002300
	GO TO 508	PL002310
507	CONTINUE	PL002320
	CALL SYMBOL (X+1.,Y-1.,4,.'J-',0.,2)	PL002330
	RNSE@ =-FLOAT(NSE@(L))	PL002340
	CALL NUMBER (X+8.,Y-1.,4,RNSE@,0.,-1)	PL002350
	GO TO 508	PL002360
508	CONTINUE	PL002370
C		PL002380
	500 CONTINUE	PL002390
	IS#=1	PL002400
	GO TO 470	PL002410
509	CONTINUE	PL002420
	REWIND ITAPEP	PL002430
	CALL PLOT (XLEN+50,0,0.,-3)	PL002440
	CALL PLOT(0.,0.,777)	PL002450
		PL002451

Appendix 4. (continued)

FACOM 230-75 (M7)

L I B E 77.11.21 (V-03 L-12)

79/05/29

PAGE-0007

SOURCE ELEMENT LIST (8BIT MODE)

	CALL PLOT(0.,0.,888)	PL002452
	CALL PLOT(0.,0.,666)	PL002453
C		PL002460
	400 CONTINUE	PL002470
C		PL002480
	999 CONTINUE	PL002490
	CALL PLOT (0.,0.,999)	PL002500
	RETURN	PL002510
	END	PL002520